United Nations Educational, Scientific and Cultural Organization
GRÓ GTP Geothermal Training Programme Under the auspices of UNESCO

GRÓ GTP, Grensásvegur 9,
IS-108 Reykjavík, Iceland

Reports 2021
Number 8

BERLÍN HIGH TEMPERATURE GEOTHERMAL SYSTEM, EL SALVADOR: EVALUATION OF GEOSCIENTIFIC INPUT FOR A CONCEPTUAL MODEL AND A NEW WEIGHTED MODEL WITH QUANTIFICATION OF FAVOURABLE DRILLING TARGETS

Mayra Raquel Hernández
LaGeo S.A. De C.V.
15 av. Sur, Colonia Útila
Santa Tecla, La Libertad
EL SALVADOR
mhernandez@lageo.com.sv

ABSTRACT

A weighted model of the most favourable drilling targets in the Berlín geothermal field in El Salvador has been developed. It is based on the last updated conceptual model, new interpretations, and new models created with the Leapfrog Geothermal program. Previous data have been interpreted and updated to a digital format to be integrated into a 3D model. The main 3D models are presented in this report, their correlation, and integration into the weighted model. Additionally, the modelling approach and methods are briefly discussed. The purpose of the weighted model is to better understand the nature and characteristics of the geothermal system to minimize risks associated with future drilling targets. It presents an objective estimate of the most favourable drilling targets according to available geoscientific results. The various datasets provide the basis for the weighted model, which are primarily sub-divided into four groups: a) surface data, b) well data, c) well logs, and d) other types of data like the 3D resistivity model. The resulting workflow describes how to bring together multidisciplinary interpretation results, highlighting areas of uncertainty and the required future work. The weighted model suggests eight different drilling targets where the best parameters converge from all models, indicating a favourability equal to or higher than 85%.

1. INTRODUCTION

The geothermal activity in Central America is associated with the local subduction zone, where the Cocos Plate sinks underneath the Caribbean Plate at the Middle America Trench. The subduction pushes crustal rocks to great depths, while magma and heat are transferred towards the surface (DeMets, 2001). The subduction area is seismically very active due to rapid plate convergence, which also creates numerous different volcanoes, and in many cases, high-temperature geothermal systems with great energy production potential, like in El Salvador.

In 2020, the total electrical energy generated from geothermal resources in El Salvador was 1,450 GWh, representing 26% of the total electrical energy utilization (Unidad de Transacciones S.A. de C.V., 2020).

However, LaGeo (Geothermal company in El Salvador) aims at increasing the installed capacity from geothermal resources. Currently, there are two geothermal areas at the feasibility stage: San Vicente with 36 MW_e and Chinameca with 50 MW_e estimated power potential, respectively (LaGeo, 2021a). Including the already exploiting geothermal areas in Ahuachapán (installed capacity of 95 MW_e) and Berlín (installed capacity of 109.2 MW_e) and other potential geothermal areas, explored and recognized, the total estimated geothermal potential in El Salvador is ~600 MW_e, of which 235 MW_e are estimated for the Berlín geothermal field (LaGeo-SIGET, 2012).

Geothermal energy plays an important role in the energy sector of El Salvador. In addition to electricity generation the resource has been utilized for different direct applications throughout the country's history. The direct uses include thermal medical-bathing, drying coffee, pasteurization of milk, candle making, and cooking food by local people living nearby the geothermal areas (Asunción and Pabón, 2019).

Different scientific disciplines have been applied to develop and update the conceptual model of the Berlín geothermal field, which aims to characterize the geothermal system of the area and reduce risks in well-targeting. At the moment, the only quantitative input to evaluate production potential of possible areas has involved the application of numerical models. However, it is essential to observe anomalies supported by different datasets to understand the nature of the geothermal system that permits identifying the most promising drilling targets of the area quantitatively.

In this study, a weighted model of the Berlín geothermal field is developed based on the last update of the conceptual model and other 3D models created using Leapfrog Geothermal, allowing an estimated quantification of the most promising drilling targets of the area.

2. BERLÍN GEOTHERMAL FIELD

2.1 Current status of the Berlín geothermal field

The Berlín geothermal field is located at 258,000 – 274,000 m latitude and 547,000 – 559,000 m longitude in El Salvador (Figure 1). In the geothermal power plant, there are three condensing units: two units of 28 MW_e (Unit 1 and Unit 2) installed in 2000, and one of 44 MW_e (Unit 3) operating since 2007. In addition, there's one binary unit of 9 MW_e (Unit 4) operating in Berlin since 2009. The system is connected to 40 wells of which 16 are production wells, 20 are hot injection wells, and 4 are ambient temperature injection wells (Monterrosa and Santos, 2013).

Over the past 29 years (1992-2021), the Berlín geothermal field has been in commercial operation through several stages of development. Currently, the installed capacity is 109.2 MW_e and the total mass extracted is around 890 kg/s (data registered in September 2021). The separated water is injected in three different ways: 1. A fraction of the separated water is injected at high temperatures (~ 172-180°C), transported directly from the separators to the reinjection wells; 2. Some water is injected at 140°C after transferring heat to the working fluid (isopentane) of the binary unit, and 3. The water is injected at lower temperature (60°C) by gravity or pumps (LaGeo, 2020a).

The production and reinjection wells range from 1,085 m (TR-18A) to 2,690 m (TR-17A) depth and 503.8 m (TR-11A) to 3,455 m (TR-19C) depth, respectively. Figure 1 shows the location of wells and the power plant location as well as the main fault system.

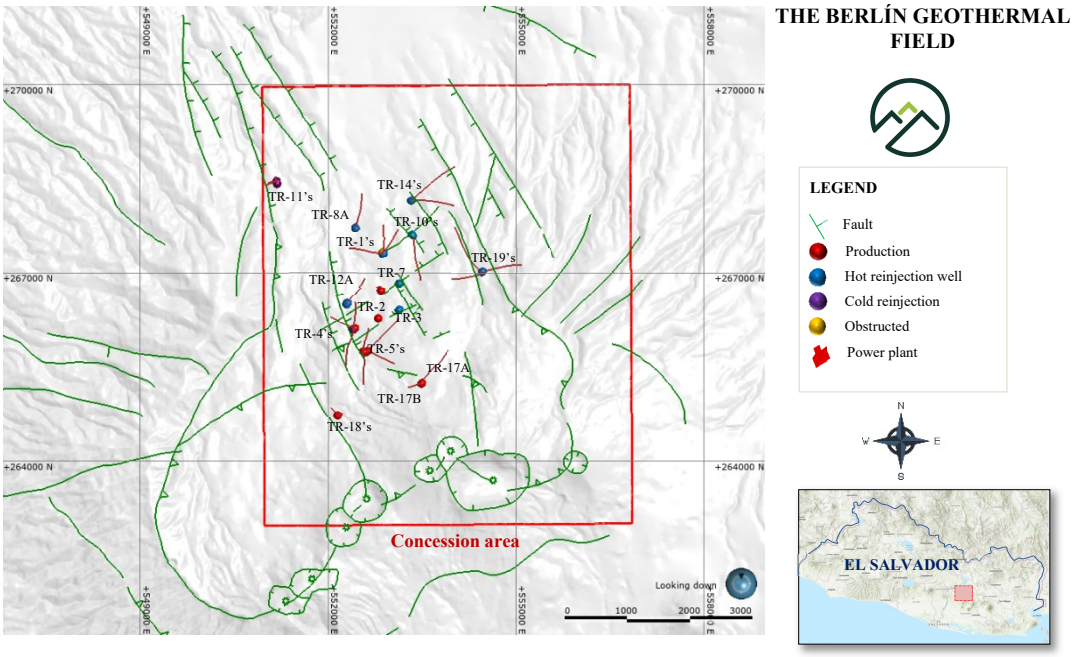

FIGURE 1: The Berlín geothermal area. The map shows the main fault system (green lines) inferred by aerial photographs and superficial exploration, the concession area awarded by Superintendecia General de Electricidad y Comunicaciones, SIGET (red square), and the different types of geothermal wells drilled in the area (modified from LaGeo, 2019). The inset map shows the location of the geothermal area in El Salvador

According to LaGeo Sustainability Protocol (LaGeo, 2011), the capacity factor indicates the utilization of the geothermal plant during a specific period (annual evaluation). In the case of the Berlín geothermal field, which is liquid-dominated, the exploitation history indicates a decreasing capacity factor (>90%) because of three main reasons: 1) declination of the discharge enthalpy of wells due to vaporization in the production wells and two-phase zone; 2) pressure drop due to skin formation in the production and reinjection wells; and 3) depressurization in reservoir due to excessive concentration of production wells (LaGeo, 2020b).

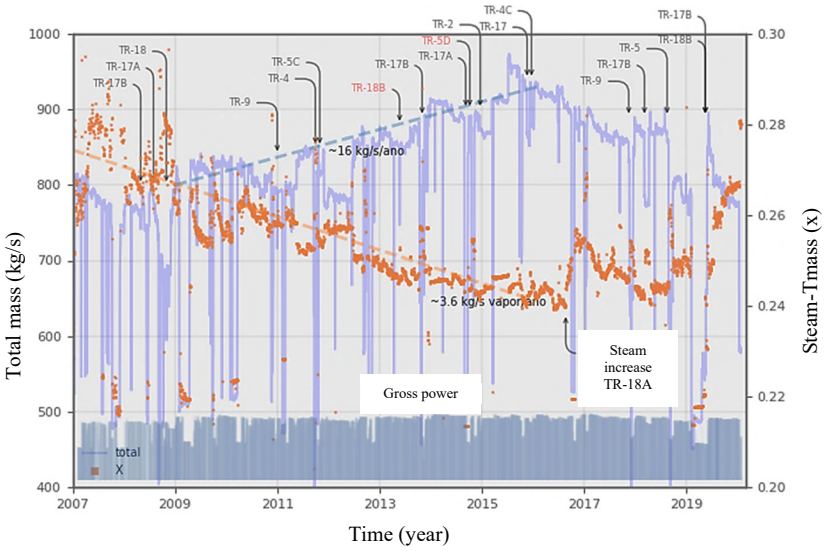

FIGURE 2: Declination of steam fraction, stimulation of production wells, and mass increase with condensing Unit 1, Unit 2, and Unit 3 operating (modified from LaGeo, 2020b)

To avoid the declination of the enthalpy it is necessary to increase the extraction of the mass; however, items 2 and 3 above mean a decrease in the flow, although the skin in the wells could be solved through chemical cleaning. Regarding item 3, it would be advantageous to aim for equilibrium in the extraction-recharge by expanding the production-injection zones in the area (LaGeo, 2020b).

Figure 2 shows the cooling effect of vaporization reflected by declining steam ratio and total mass (Equation 1). In this case, "x" is a function of enthalpy and separation pressure. This means that it is necessary to extract more mass from the wells connected to Unit 1, Unit 2, and Unit 3 to maintain a high-capacity factor (>90%).

$$x = {}^{mass\ of\ steam}/_{total\ mass} \quad \text{[dimensionless]} \tag{1}$$

In the main production area, the extraction is higher than the reinjection, causing declining reservoir pressure. Accordingly, preferable new drilling targets are outside the principal area of production and reinjection (LaGeo, 2020b). Figure 3 shows the site proposal for production wells, primarily to the east, west, and south of the current geothermal field. These areas are referred to in the last conceptual model report for the Berlín geothermal field (LaGeo, 2019).

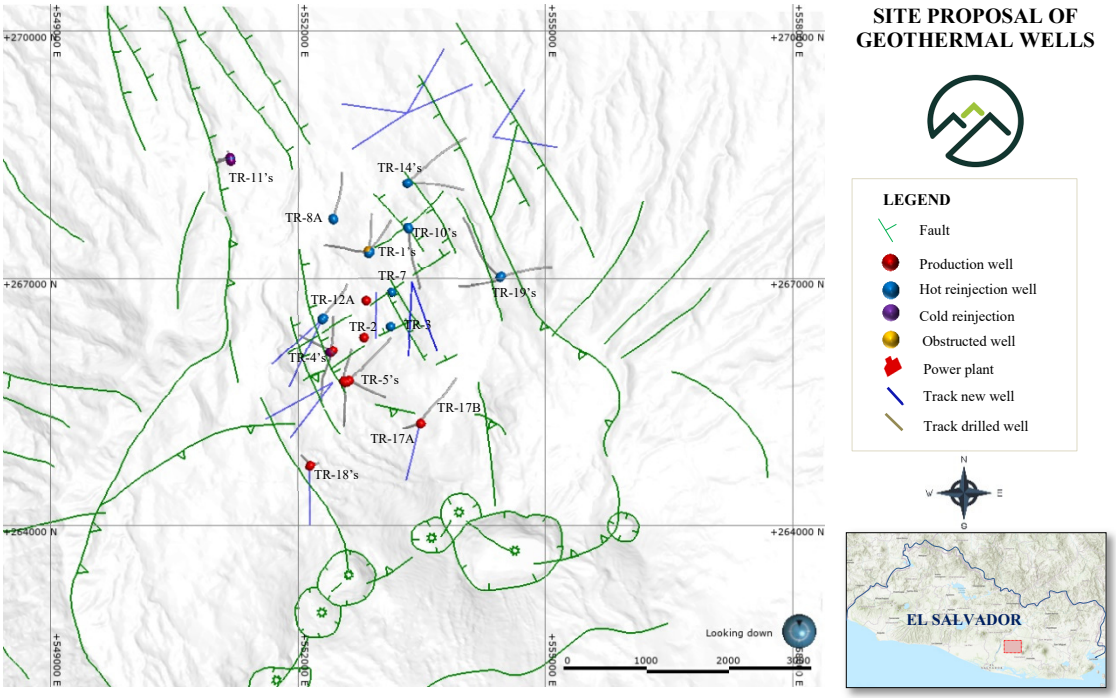

FIGURE 3: Proposed new directional geothermal wells in the Berlín geothermal field (modified from LaGeo (2019)), shown as purple lines.
The inset map shows the location of the geothermal area in El Salvador

2.2 Physical characteristics

2.2.1 Historical summary of exploration and utilization

Different studies have been carried out in the area during the surface exploration stage involving reconnaissance and pre-feasibility studies (Table 1). The studies began in the 1960s. After that, the commercial operation of the field started on a small scale in 1992 with two back pressure units of 5 MW_e each (Montalvo and Axelsson, 2000). Four years later, the first conceptual model was developed (1996), which helped locate new geothermal wells, enabling increasing the installed electrical power from 10 MW_e to 66 MW_e in 1999 (Rodriguez, 2005).

Following complimentary studies from 1996 to 2007 new drilling targets were identified, leading to an increase in installed electrical power of 44 MW_e and 9.2 MW_e in 2007 and 2008, respectively. Thereby, achieving a total installed electrical generation capacity of 109.2 MW_e (without the back pressure units).

During the next years, and after the first conceptual model, different multidisciplinary studies were carried out to characterize the geothermal system (Table 1). As a result, there are currently six updated conceptual model reports. Each one has helped identify, characterize, and update different features of the geothermal system. The last conceptual model is from 2019 (LaGeo, 2019).

TABLE 1: Geoscientific studies during the exploratory stage of Berlín

Discipline	Reconnaissance	Pre-feasibility
Geology	Geological exploration (local and regional) Laboratory work (petrography, rock dating)	Stratigraphy studies Volcanology studies Detailed cartography Laboratory studies (petrographic studies, chemical analysis of rocks, XRD and rock dating) Structural geology
Geochemical	Surface manifestations (mapping) Temperature in superficial fluids Geothermometry	Complementary studies of surface manifestations (thermal sources) Laboratory (geothermometry, mixing fluids models, isotope hydrology)
Geophysical	Gravity studies (regional) Vertical electrical soundings (VES)	Complementary gravity studies Magnetic studies Magnetotelluric and TDEM resistivity studies

It is essential to mention that through the contribution of each consequent geoscientific study it has been possible to drill 40 geothermal wells, or 16 production wells and 24 reinjection wells. In addition, although direct use is not the primary use of geothermal energy in El Salvador, the geothermal resource has been used in different ways. For example, direct uses such as thermal medical baths, coffee drying, milk pasteurization, candle making, and cooking of food have been implemented by the local population living in areas surrounding the geothermal areas (Asunción and Pabón, 2019).

2.2.2 Geological overview

The Berlín geothermal field is located at the southern flank of the central graben traversing El Salvador and in the northwest sector of the Berlín-Tecapa volcanic complex. The volcanic activity of the region is related to the tectonic interaction between the Cocos and Caribbean plates in the subduction zone (DeMets, 2001).

The Berlín-Tecapa volcanic complex is a stratovolcano where lava flows, pyroclastites, and epiclastites alternate, mainly andesitic, and basaltic-andesite rocks (LaGeo, 2019). The area is composed of several volcanic cones surrounding the area, specifically to the SE of the old volcano of Berlín. The main geological formations from the youngest to the oldest are shown in Figure 4.

Through photogeological studies and LandSat satellite images, the lineaments or fault systems have been classified into three groups (LaGeo, 2019):

1. NW-SE is the orientation of the area's youngest, most active, and most prominent fault system, associated with the structures through which geothermal fluids rise to the surface layers. The faults are mainly normal faults.
2. NE-SW is the orientation of a less visible system in the area which is associated with reverse faulting.
3. N-S and W-E striking directions are associated with strike-slip faults with a small normal component.

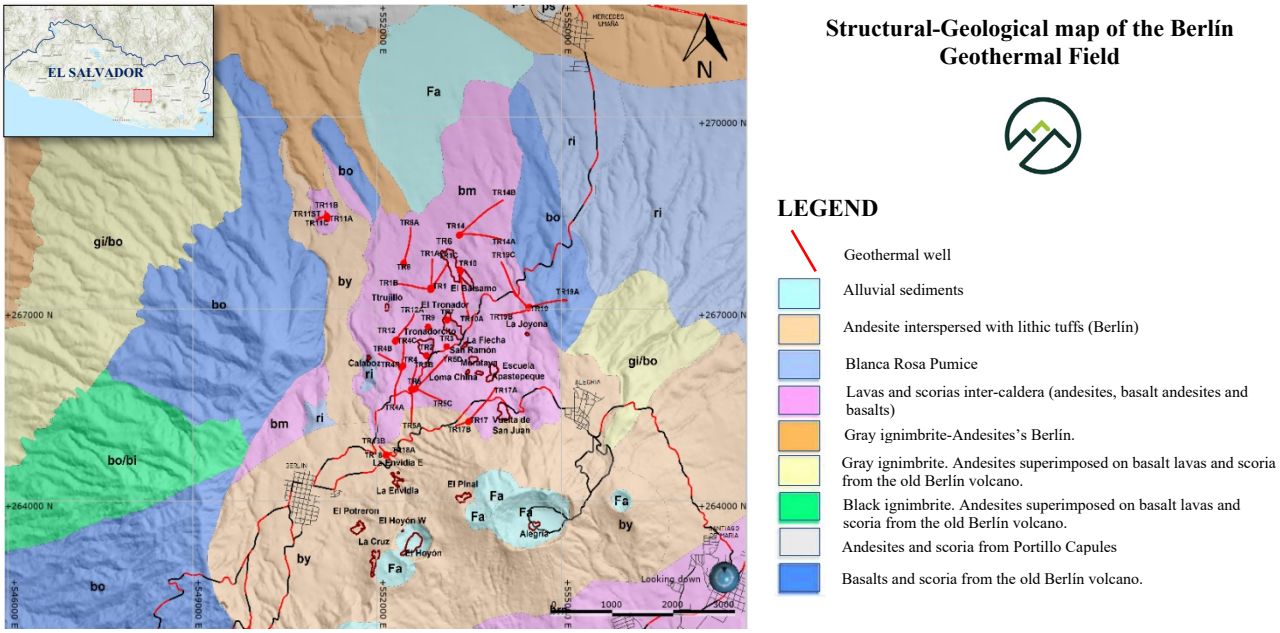

FIGURE 4: Geological map of the Berlín geothermal field (modified from LaGeo, 2019). The inset map shows the location of the geothermal area in El Salvador

2.2.3 Geochemical overview

The high concentration of H_2 in fumaroles in the southern part of the field is related to the high temperature in the volcanic complex of Berlín-Tecapa (LaGeo, 2019). The high concentration of this gas is due to the magmatic degasification process. In addition, the isotopic composition in the wells located in the south part indicates an equilibrium temperature between 340 and 350°C. Therefore, based on various information like geo-volcanology, H_2-content, and the temperature measured in the wells, the up-flow zones are believed to be close to the TR-17 and TR-18 platform and TR-4 and TR-5 platform (LaGeo, 2019).

The reservoir is considered to be a saline aquifer with chloride-sodium neutral characteristics. It has fissured tuff and andesite lavas with high hydrothermal alteration (propylitic facie). According to the cation and gas geothermometers, the temperatures lie between 260 and 300°C and 340 and 350°C, respectively. Figure 5 shows the relationship between chlorine and boron in some of the production wells in the area where it is possible to observe differences between the physical processes of the geothermal fluids (LaGeo, 2019). For example, in wells TR-2, TR-3, TR-9, and TR-17 boiling takes place, while in well TR-18 dilution occurs due to mixing of water at great depth. However, fluid in all production wells have the same origin according to the linear correlation shown in Figure 5.

Geochemical studies have helped define two up-flow zones: the characterization of fluids emanating from a fissure formed in 2013 in the crater of the El Hoyón volcano indicates deep fluid with temperatures around 300°C (NaK geothermometer), along with fluid in the center of the geothermal field (TR-4's zone) with similar characteristics (LaGeo, 2019).

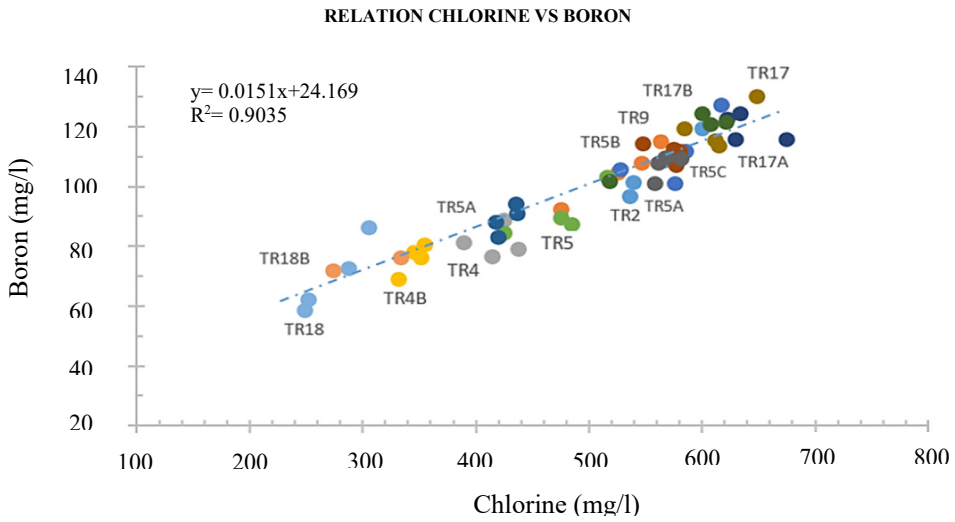

FIGURE 5: Relationship between chlorine and boron concentration in the production wells (LaGeo, 2019)

2.2.4 Geophysical overview

According to the latest conceptual model report for the Berlín geothermal field from 2019, different geophysical surveys have been carried out (LaGeo, 2019). During 2012-2019, a new 3D resistivity model was created using 13 additional MT soundings located in the center, northwest, and south of the field. However, only insignificant differences have been identified between the new 3D model and the previous one based on 1D inversion, they are in general similar and show the same trend (LaGeo, 2019).

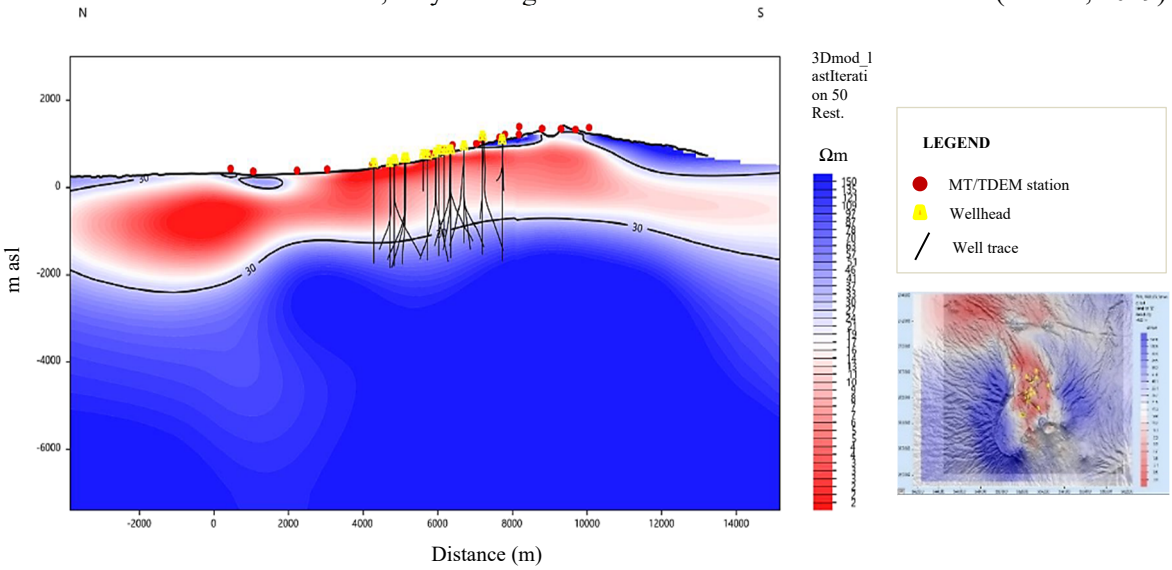

FIGURE 6: A N-S trending resistivity cross-section based on 3D inversion of MT data. The cross-section shows the 30 Ωm contour that represents the top of the reservoir (black contour), the smectite cap above the reservoir with resistivity < 10 Ωm, the location of the geothermal wells close to the profile (black traces) and the MT/TDEM soundings (red circles) (LaGeo, 2019)

Figure 6 shows a N-S striking resistivity cross-section based on 3D inversion of MT data with three main layers; a low-resistivity layer associated with altered clay minerals (smectite) and resistivity < 10 Ωm; a transition zone of the geothermal system with resistivity between 10 and 30 Ωm; and the reservoir with resistivity between 30 and 90 Ωm extending to the south of the production zone (LaGeo, 2019).

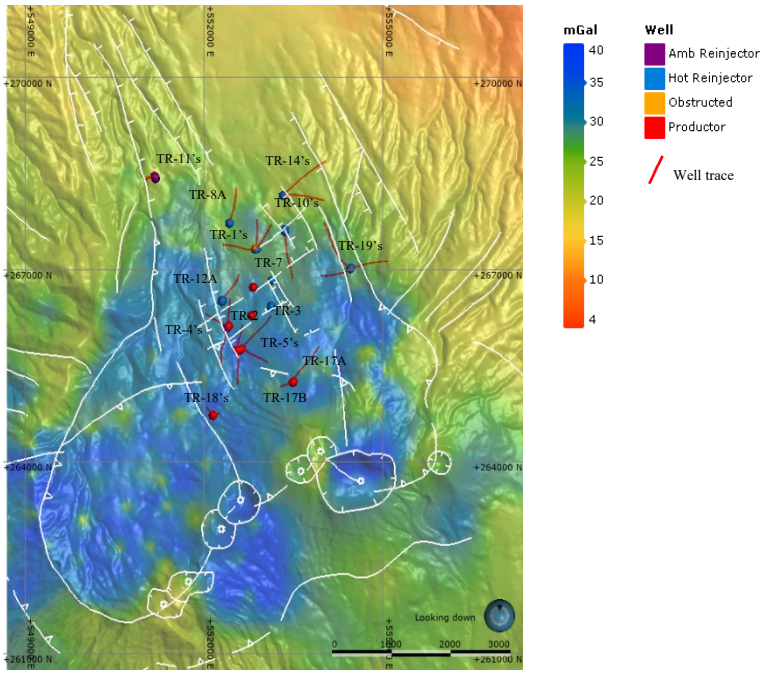

FIGURE 7: Bouguer gravity map, using the density ρ = 2.3 g/cm^3 for Bouguer and terrain correction (LaGeo, 2019)

Figure 7 shows the Bouguer gravity anomaly map that reveals profound gravity variations. The main aspect that can be observed is the high gravity values to the southwest, south, and close to the geothermal wells. It has been proposed that the high values are limited in the north by the boundary of the old Berlín caldera; however, this boundary is not visible on the surface. In the north, the limit is close to wells TR-9 and TR-1 (LaGeo, 2019).

On the west and east side, the limits are represented by the Berlín caldera boundary and La Calzadora fault, and Guallinac fault, respectively (LaGeo, 2019).

From 2013 to 2019 seismicity in the area was recorded. The results were compared with the resistivity model based on 1D inversion (see Figure 8). The possible presence of a body with ductile properties at approximately 6,000 m b.s.l. was identified which is consistent with the deep conductive anomaly and assumed to be related to the heat source of the geothermal system (LaGeo, 2019).

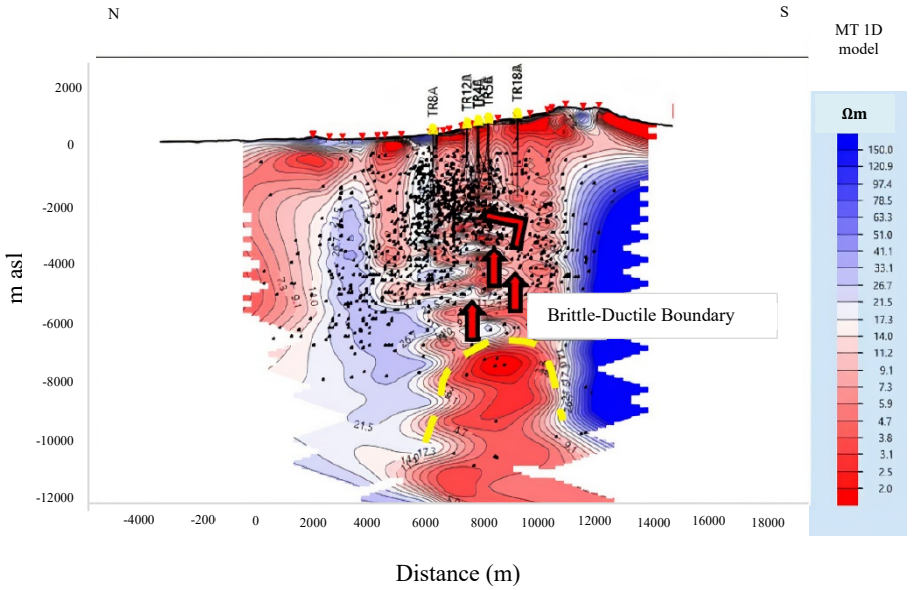

FIGURE 8: Comparison between the resistivity model based on 1D inversion and earthquake location, recorded in 2013-2019 – N-S profile. Red arrows indicate the up-flow and the dotted yellow line the brittle-ductile interface (LaGeo, 2019)

2.2.5 Geothermal surface manifestations, an overview

Fumaroles are surface manifestations that indicate high temperature and flow at depth. From the fumaroles on the surface, it is possible to evaluate the physical and chemical processes at great depth (Wilson, 1960).

In Berlín geothermal field, 21 fumaroles have been monitored (Figure 9). They are located in the southern, central, and northern part of the area. The fumaroles in the volcanic area have an acidic pH composition (associated with the up-flow). In the south, the fumaroles show neutral pH composition and are in the surrounding of the high-temperature wells; and in the north, the fumaroles are associated with the discharge and have an intermediate pH composition (LaGeo, 2019).

In 2018, the Tronador fumarole, located in the northern part of the field, showed the highest measured temperature which was 98.9°C. This could be associated with the entry of primary steam from a source of geothermal fluids at greater depth. The fumaroles El Hoyón (96°C) and La Laguna de Alegría (93.8°C) are of deep origin with magmatic influence (LaGeo, 2019).

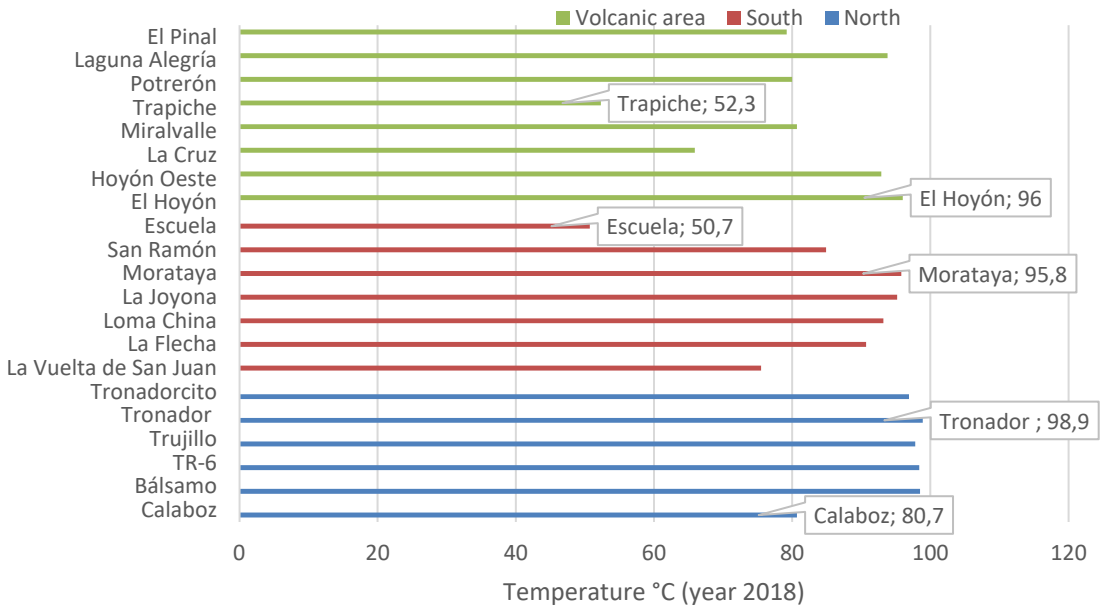

FIGURE 9: Temperature of Berlín fumaroles measured in 2018. The fumaroles are divided into three groups: the volcanic area (green color), southern area (red color), and northern area (blue color). The labels show the maximum and minimum values for each group of fumaroles

2.2.6 Data from wells in the Berlín area

Lithological data

During the period from 2012 to 2018, four production wells were drilled which have been included in the new conceptual model. The lithology is divided into four lithological units (I-IV) based on thin section analysis using microscopic analysis as well as macroscopic and microscopic analysis of cores from 27 wells (LaGeo, 2019).

The principal types of rocks are andesite or andesite-basaltic lavas, pyroclastic rocks like tuff, and ignimbrites. Unit I is made up of superficial materials, e.g., andesite lavas alternating with some pyroclastic rocks. This unit has high permeability corresponding to the superficial aquifer. The thickness

of Unit I is between 400 and 990 m. Unit II is made up of pyroclastic rocks with secondary fissures, Unit III is related to tuff, and Unit IV is made up of andesitic lava and corresponds approximately to the geothermal reservoir (LaGeo, 2019).

Alteration mineral facies

The hydrothermal alteration in geothermal fields is different in different types of reservoir rocks (Kristmannsdóttir, 1985). The intensity or degree of alteration is related to several factors such as permeability (related to the gas content and hydrology of the system), rock composition, temperature, duration of the activity, temperature/pressure, hydrothermal fluid composition, and hydrology (Kristmannsdóttir, 1985; Browne, 1978; Reyes, 2000; Franzson, 2008).

In high-temperature geothermal fields in Iceland, the pyrite mineral is associated with permeable zones (Kristmannsdóttir, 1979), but in Berlín geothermal field, the pyrites and zeolites are associated with permeable zones at intermediate temperature (150-220°C) (LaGeo, 2019). However, between -900 and -1900 m a.s.l. (thickness of the deep reservoir) pyrites and epidote minerals have been identified. The pyrite minerals correspond to permeable zones at high temperatures (230-260°C).

The analysis methods used to determine hydrothermal minerals of alteration are petrographic microscope and X-Ray diffraction analysis (LaGeo, 2019). In general terms, the hydrothermal alteration in Berlín is characterized by secondary minerals like:

- cristobalite, quartz and zeolites,
- clays and chlorites,
- epidote,
- calcite,
- oxides and hydroxides, and
- sulfides.

The hydrothermally altered rocks are grouped into six principal facies, argillic, argillic-phyllic, phyllic, phyllic-propylitic, propylitic, and potassic. Generally, each type of alteration represents a stabilized temperature according to the different types of identified minerals (LaGeo, 2019).

The argillic facie clay minerals, such as smectite and zeolites, are altered at low temperatures (stabilized temperature between 50 and 150°C). The argillic-phyllic facie clay minerals, like quartz, calcite, and zeolite, are altered at a stabilized temperature of 150-180°C. The phyllic facie, the same minerals as the previous facie, is altered at higher stabilized temperature (200-230°C). The formation of epidote minerals happens in the phyllic-propylitic facie as well as chloride. The stabilized temperature in this facie is 230-260°C. The propylitic facie is characterized by high content of epidote deposited in fissures; also, it is associated with minerals like quartz, calcite, and other minerals at high temperatures. Stabilized temperatures are estimated between 260 and 300°C (LaGeo, 2019).

Temperature

From 40 geothermal wells (production and reinjection wells), only 31 PT profiles were available for the construction of the formation temperature model of the Berlin geothermal reservoir. This is because, in some reinjection wells, the time allowed for thermal recovery was affected by the urgency of injection during the first year of the field development. For that reason, data from wells TR-1B, TR-1C, TR-8A, and TR-11ST are not available (LaGeo, 2007).

According to the updated formation temperature in Berlín, three main zones have been identified for future development; the first one corresponds to the biphasic and saturated steam zone intercepted by wells TR-18 and TR-18A; the second one is the zone intercepted by wells TR-2, TR-3 and TR-17A; and the last one is the deep reservoir close to site of well TR-4, drilled with the aim of increasing the

production (LaGeo, 2007). Figure 10 shows the formation temperature distribution and the three main zones of potential development (R1, R2 and R3).

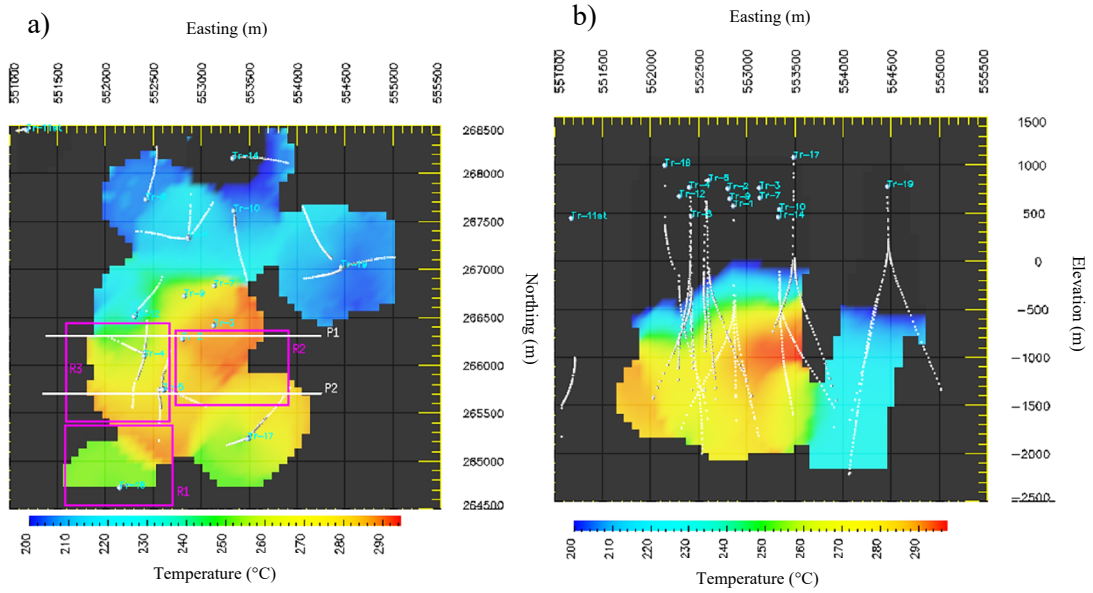

FIGURE 10: a) Temperature distribution at 100 m a.s.l. delineating three zones of potential development in Berlín (red boxes), and b) temperature distribution along a WE laying profile (LaGeo, 2007)

3. WEIGHTED MODEL AND QUANTIFICATION OF FAVOURABLE DRILLING TARGETS IN THE AREA

Leapfrog Geothermal with the Edge extension is the modelling program used in this project. According to Leapfrog website (Leapfrog, 2021a), the software is a 3D implicit modelling tool and workflow tailored for geothermal experts, in their words "Leapfrog Geothermal is an intuitive, workflow-based 3D subsurface modelling software that enables you to build and refine models very quickly".

In this case, the software allows to build surfaces for different types of models with two different interpolants: the RBF interpolant if the data are from wells, and Inverse Distance Weighted (IDW) grid interpolant for resistivity data. Each type of interpolant will be explained in the next sub-section.

After building the models with different interpolants, combined models, and some block models, the weighted model is created to quantify the most favourable drilling targets in the area. within this study an academic license of Leapfrog Geothermal with the "Edge" extension was used, which helps to check the estimates produced for blocks and inspecting the data used to create the model.

The weighted model is created from calculations based on the block model. Calculations use estimators and data to derive new values representing the quantification of favourable drilling targets in the area (Leapfrog, 2021b).

3.1. Methods and data

As briefly mentioned in the introduction to this work, a weighted model for the Berlín geothermal field is developed based on the most current update of the conceptual model and other 3D models created in Leapfrog Geothermal, allowing the identification of the most promising drilling targets of the area. In

addition, there are other technical reports with results from different geological, geochemical, and geophysical exploration studies. Some of the reports are only available for internal LaGeo use; however, it has been possible to use some of these results and data for the weighted model. Following is a description of the development process, used to construct the weighted model.

First is important to start with the acquisition and preparation of the data to create the basis for the work that follows. Then, following the limits of the global data, the general boundaries of the model are determined. The area of the weighted model is 21 km^2.

3.2. Workflow

The surface data were imported as shapefiles and several maps of the area geo-referenced for correlations with the data. Depths and thicknesses of lithological units, alteration minerals, temperature, and pressure were obtained from well logs. Finally, the data were organized in tabular format (including the seismic data) to be imported into the Leapfrog Geothermal database.

The workflow that was developed through the weighted model for the Berlín geothermal field is comprised of five main steps (Figure 11).

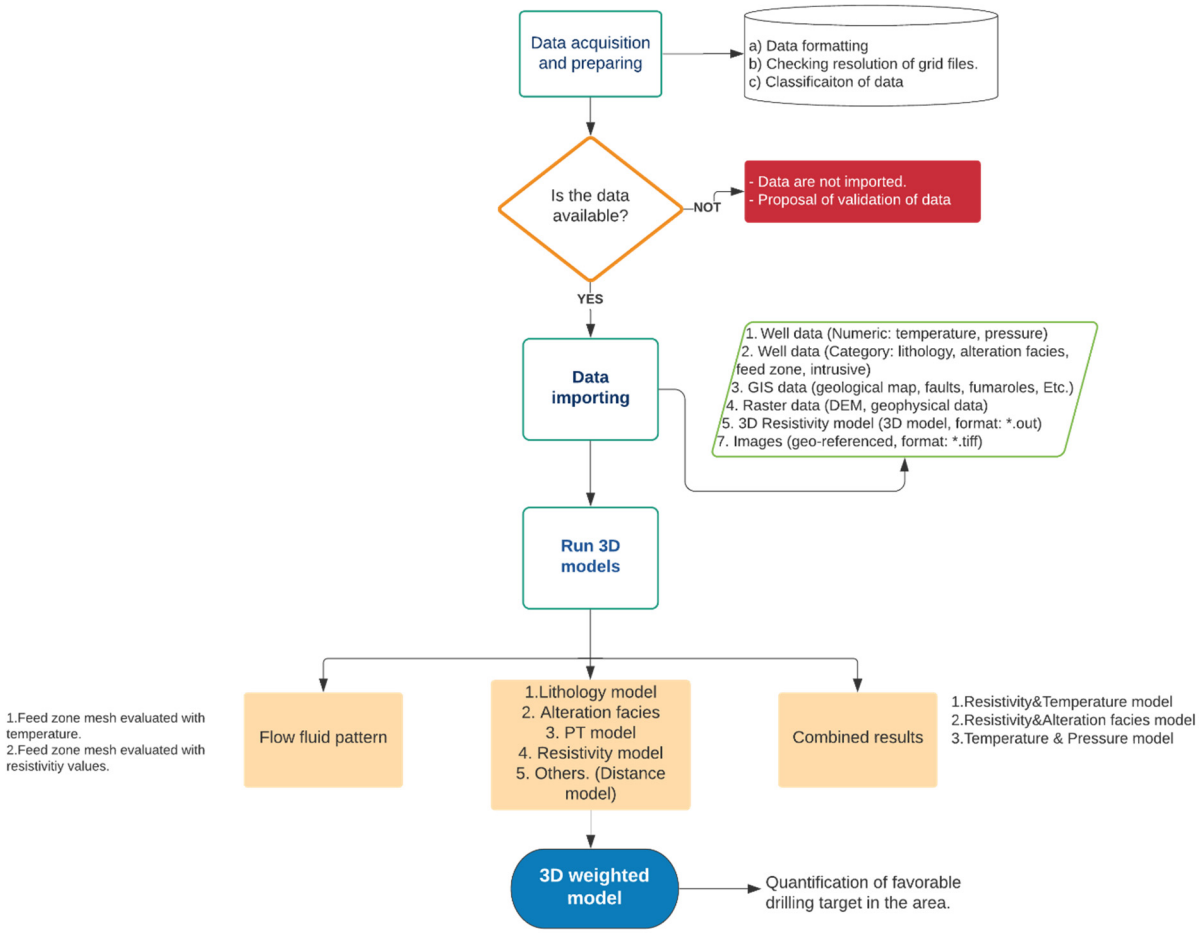

FIGURE 11: Workflow step diagram utilized to create a 3D weighted model for Berlín. This process may change with the acquisition of new data

3.3 Input data

Since the last conceptual model was published in 2019 (LaGeo, 2019), some additional measurements and interpretations have been carried out concerning the geothermal area, such as seismic tomography (work in progress) and chemical studies. However, most of the data and information used in this work have been taken from the previous report to create the 3D base models that are the input into the weighted model. The 3D models are new results in a three-dimensional view. They allow for new interpretations and correlations that support some of the hypotheses that have already been put forward by LaGeo's experts, suggesting some relevant aspects of the geothermal system.

The workflow process for each model is described in the following sections. Additionally, new 3D models and interpretations are proposed that will support and help the elaboration and updating of the Berlín conceptual model.

Different types of data were used for this project. The information and data manipulation were applied in the process of constructing the 3D weighted model. Table 2 shows the four types of data imported into Leapfrog.

TABLE 2: Overview of different types of data imported into Leapfrog Geothermal.

Data	Explanation
Surface	Topography, surface geological maps, gravity maps, GIS data (fault system, fumaroles, MT/TDEM sounding points)
Well	Lithology/hydrothermal alteration facies, location of feed zones, wellhead location, and well survey information (well track, vertical/directional wells)
Well logging	Stabilized PT logs and current static PT logs
Others	3D resistivity model (based on MT data), location of seismic hypocentres

3.4. Modelling results

In this part, the input data described in sections 3.2 and 3.3 will be presented in different ways and with different 3D interpolants: RBF interpolants, IDW interpolants, maps, and cross-sections. Each result is the product of working with the data gathered in this project and the different ways it can be used to build a new 3D model in Leapfrog Geothermal.

3.4.1 Lithology model

The lithology was discussed briefly in section 2.2.6. The lithology model was built in Leapfrog Geothermal, using a table with four categories at different depth ranges. Figure 12 shows the proposed model as a general interpretation of the movement of the rock blocks formed due to the activity of the three principal fault systems, the old Caldera of Berlín (north area) and Blanca Rosa caldera (south area) boundaries.

The method used to generate the 3D lithology model is described in this section. Drill cuttings were analysed during the drilling period using optical microscopy of thin slices and macro/microscopic analysis of 27 cored wells in 2012. In 2020, the litho-stratigraphy was evaluated again to minimize errors in the lithology depths. In this model cross-sections were not used. A simple categorization was applied and four lithological units identified: Unit I, Unit II, Unit III and Unit IV.

Additionally, the main fault systems were added to identify differences between the location of the lithological units in the study area. The fault systems included are NW-SE (normal faults), NE-SW (reverse faults) and the caldera boundaries (old Caldera of Berlín and Blanca Rosa Caldera).

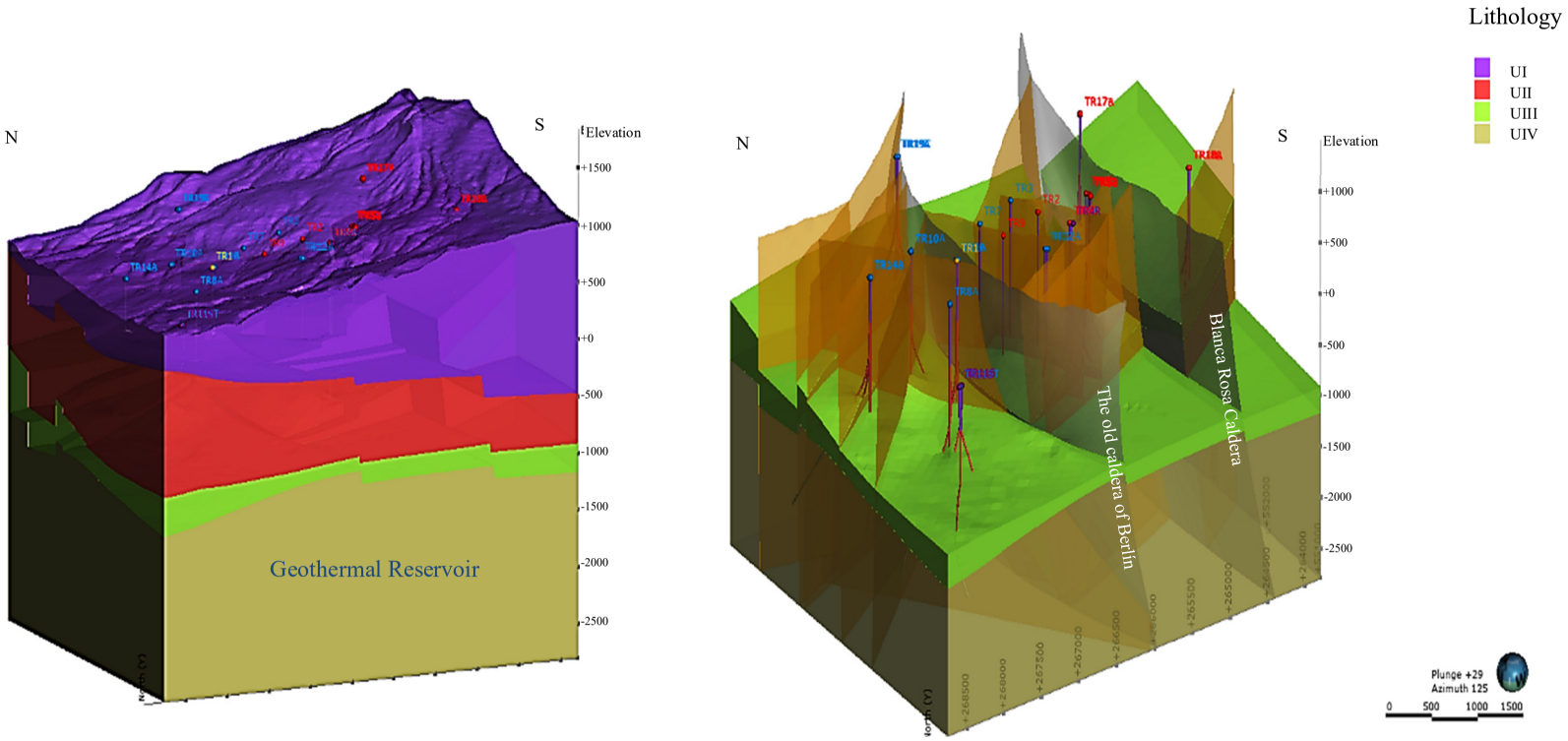

FIGURE 12: The proposed lithology model for Berlín and its interaction with the main three fault systems of the area. The model is based on well data. Unit I is made up of superficial materials, Unit II of pyroclastic rocks, Unit III is tuff related and Unit IV is made up of andesitic lava and corresponds to the geothermal reservoir

Several tracer tests have been carried out in the Berlín geothermal field. The radioactive tracers I^{131} and I^{125} were used, and they were monitored for 3-8 months. The percentage of total recovery or return of the tracer (%) has been evidenced in some wells. Chemical tracer studies indicate a connection between reinjection well TR-12A and some production wells such as TR-4C (9.4% recovery), TR-5B (2.9%), TR-9 (1.7%), and TR-5A (0.24%) (LaGeo, 2018). Thus, the most direct connection was established in well TR-4C. According to the new 3D lithological model, the fluid present in Unit IV could be influenced by the connection between the old Caldera of Berlín and La Planta fault (see Figure 13).

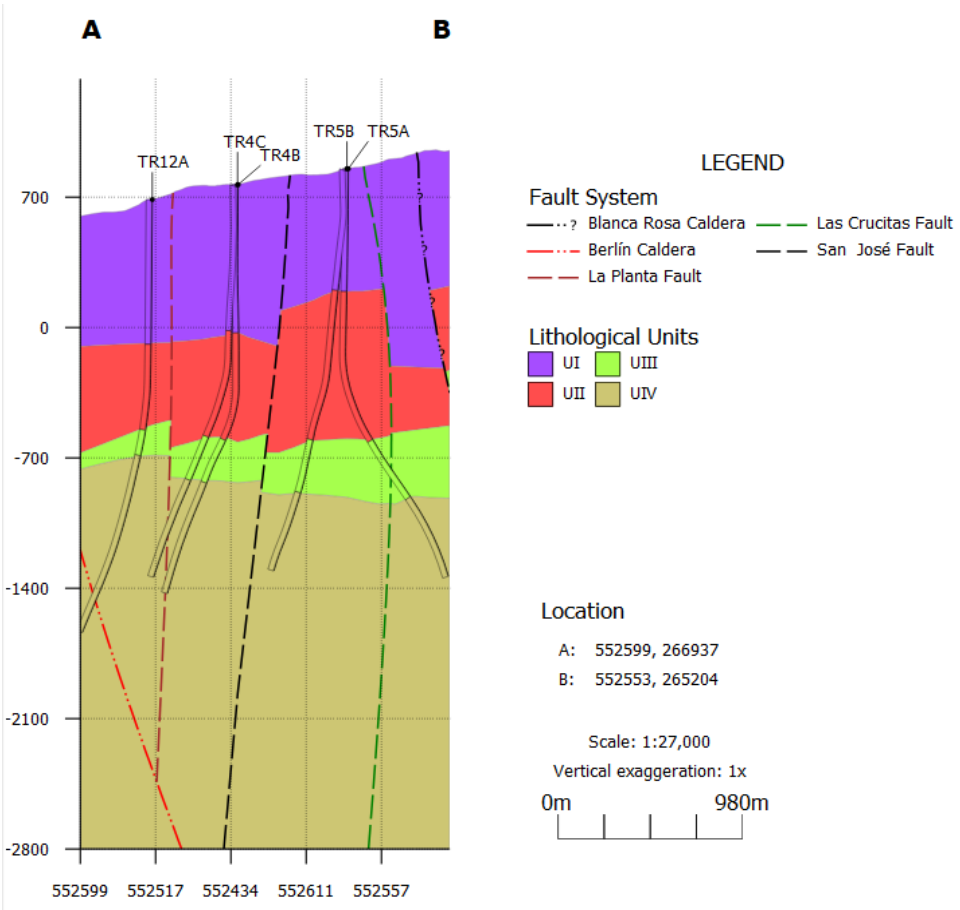

FIGURE 13: Cross-section through the 3D lithological model for Berlín including the geological fault system, based on well data. The dotted lines represent the fault system and how it intersects the model. Unit I is made up of superficial materials, Unit II of pyroclastic rocks, Unit III is related to tuff, and Unit IV is made up of andesitic lava and corresponds to the geothermal reservoir

In general terms, the lithological model shows the possible influence of the faults on the geothermal system, suggesting that the caldera structure plays an important role in the fluid flow and the fluid patterns in the area.

3.4.2 Intrusion model (granite)

Some production and reinjection wells in the eastern, northeastern, and southern part of the geothermal area intercept rocks with doleritic (small amount) and granitic composition.

These intrusions play an essential role because they are associated with a high number of fractures, indicating good permeability. For that reason, it is relevant to characterize the different parameters that describe the intrusion shape and their properties.

The intrusion model was built integrating the granite identified in wells TR-19A, TR-19B, TR-19C, TR-17A, TR-14B and TR-5A. The geological model used in Leapfrog Geothermal involved intrusions in "interval ranges from the wells". Consequently, the model was evaluated using the stabilized temperature and resistivity model (see Figure 14).

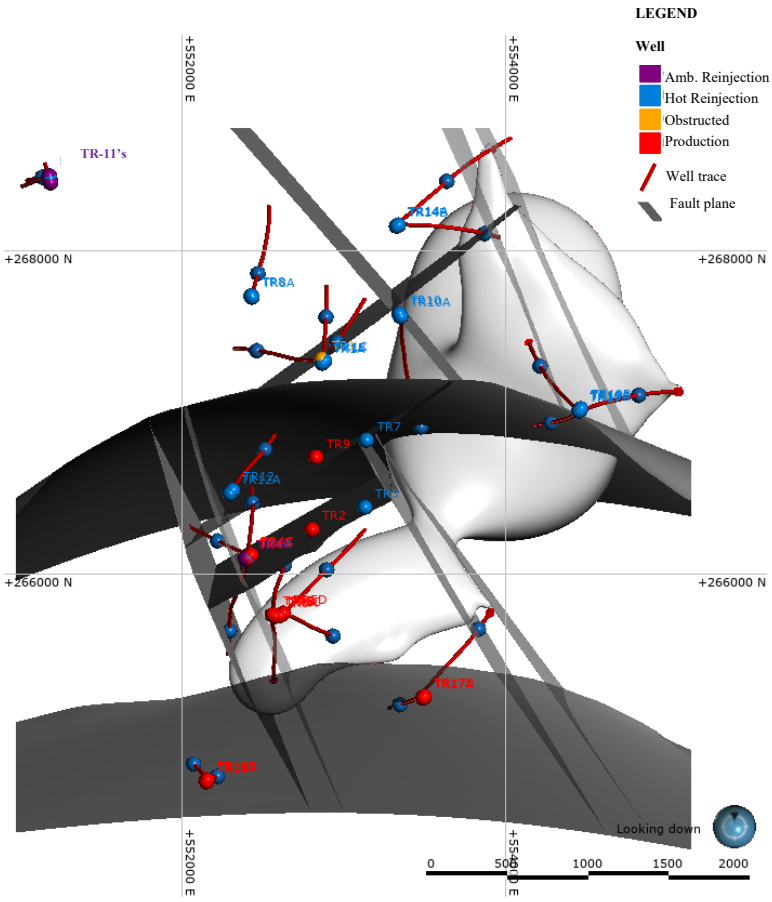

FIGURE 14: The 3D intrusion model and its interaction with several faults

Unaltered granite rocks have an electrical resistivity of around 1,000-10,000 Ωm (Giao et al., 2008). However, according to the resistivity and formation temperature models incorporated in the intrusion model shown in Figure 15, the granite is altered with resistivity values between 35 and 280 Ωm in the northern and southern part, respectively.

Also, the model is evaluated with respect to stabilized temperature. The temperature in the south (close to well TR-5) is between 260 and 307°C, possibly due to the proximity of the up-flow zone, defined according to the analysis of mineralogical assemblages (fluid inclusions), and NaKCa, and SiO_2 geothermometers (discussed in section 2.2.3). However, in the north, it is between 190°C and 210°C (close to well TR-19), suggesting a fossil heat source of the geothermal system, as there is no equilibrium with the formation temperature of minerals of the propylitic and potassic facies in this area.

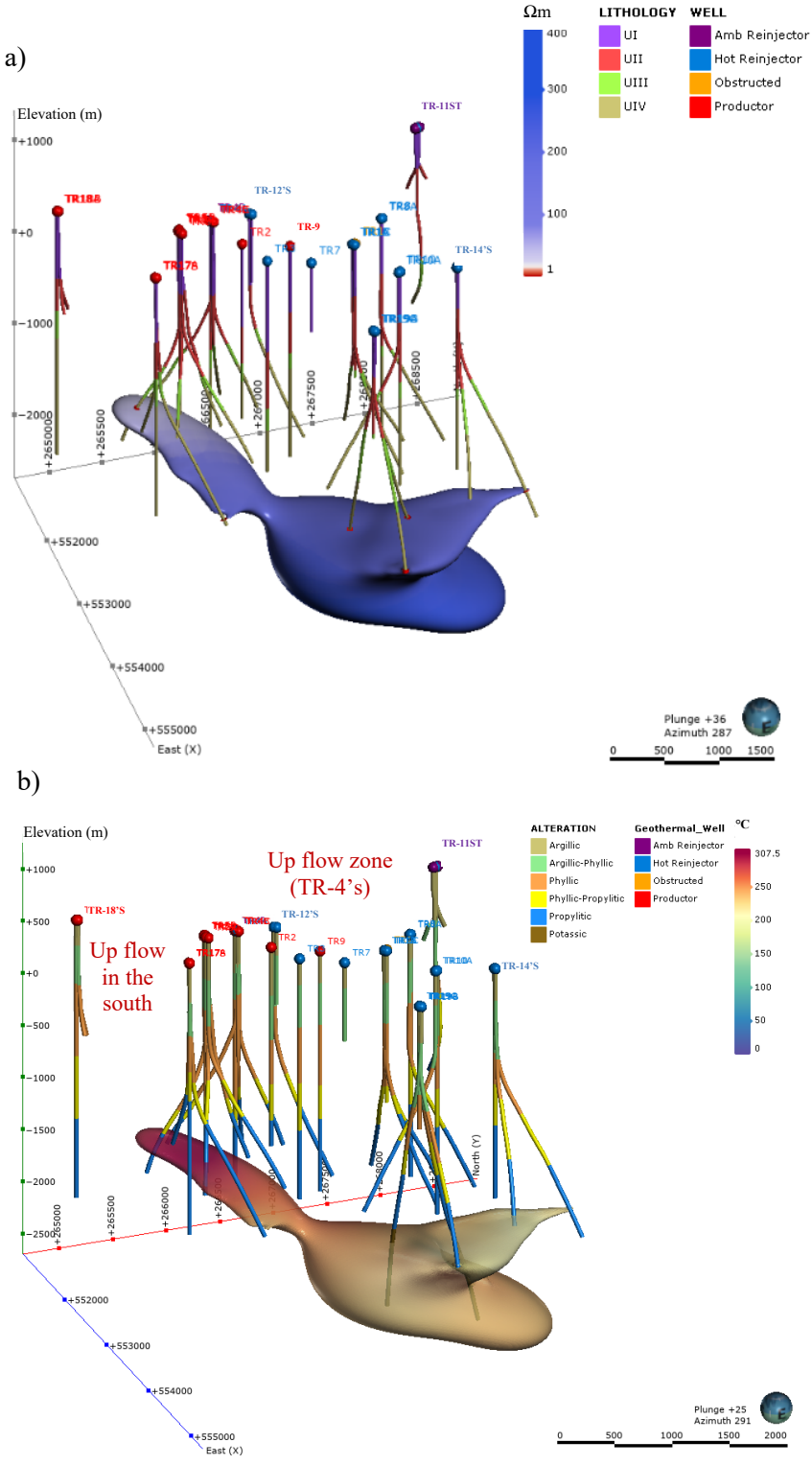

FIGURE 15: The 3D intrusion model for Berlín incorporating a) the electrical resistivity and b) formation temperature models, built in Leapfrog Geothermal. The figure legend for a) shows the lithology units and the legend for b) the alteration minerals facies

3.4.3 Structural lineament model

According to the lithological model discussed in section 3.4.1, the fault system plays an important role in the fluid flow pattern. However, for simple effects and to try to understand the rocks' movement due to the faults, the model interacts only with the NW-SE and NE-SW systems and the two caldera boundaries.

The geological structure of the old caldera of Berlín was defined according to the Bouguer gravity anomaly shown in Figure 7 (LaGeo, 2019). Blanca Rosa Caldera was inferred according to the significant difference between the lithological units in the centre and south zones which could be geological barrier effects.

Figure 16 shows both caldera collapses; however, in the south, another effect has occurred. El Hoyón and San Juan faults in the south zone of the Blanca Rosa caldera collapse suggests reverse faults forming a geological horst structure.

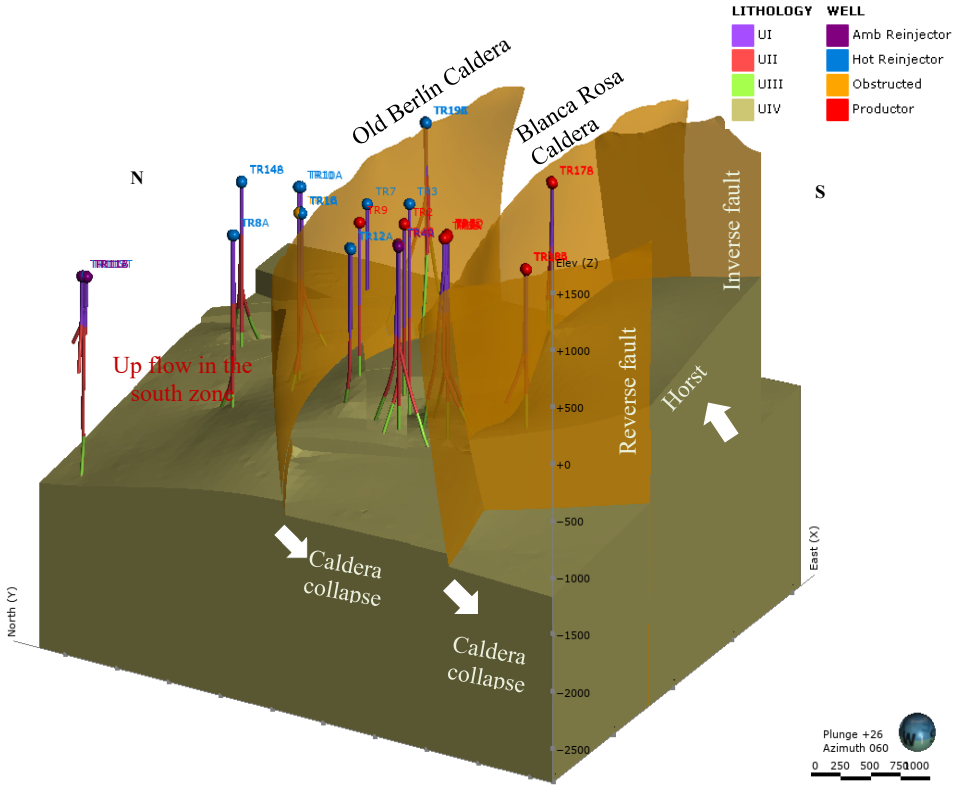

FIGURE 16: Structural system and type of geological structures in the Berlín geothermal area, based on well data. The figure legend shows the lithology units from the wells. Unit I is made up of superficial materials, Unit II of pyroclastic rocks, Unit III is related to tuff, and Unit IV is made up of andesitic lava and corresponds to the geothermal reservoir

Likewise, considering the lithological data from the wells and the motion of the rock blocks, the model suggests a faults system as described in Table 3.

TABLE 3: Structural lineaments or faults included in the 3D structural model

Fault/Lineaments	Description	Interaction type
El Beneficio	Normal fault, dip = 87.7°, azimuth=246°	Terminates at: the old Berlín Caldera and Blanca Rosa Caldera. Cross-over: San José and La Planta
Las Crucitas	Normal fault, dip = 90°, azimuth = 256°	Terminates at: the old Berlín Caldera and Blanca Rosa Caldera. Cross-over: San José and La Planta
El Tronador	Normal fault, dip = 83.2°, azimuth = 238° Compression fault	Terminates at: La Planta and Blanca Rosa caldera. Form a mini-Graben with NW-SE (inferred)
NW-SE (inferred)	Normal fault, dip = 89.03°, azimuth = 60°	Terminates at: La Planta and Blanca Rosa caldera. Form a mini-Graben with El Tronador fault
San José	Reverse fault, dip = 81°, azimuth = 326°	Terminates at: El Beneficio and NW-SE (inferred). Cross-over: Las Crucitas fault
La Planta	Reverse fault, dip = 86.5°, azimuth = 326°	Terminates at: El Beneficio and the old Berlín Caldera. Cross-over: Las Crucitas
Los Rivera	Normal fault, dip = 90°, azimuth = 233°	Terminates at: the old Berlín Caldera
Guallinac	Normal fault, dip = 85°, azimuth = 248°	Terminates at: the old Berlín Caldera
NW-SE (inferred 2)	Normal fault, dip = 83.52°, azimuth = 249°	Terminates at: Los Rivera fault
La Pila	Normal fault, dip = 87°, azimuth = 48°	Terminates at: the old Berlín Caldera
El Hoyón	Reverse fault, dip = 90°	Terminates at: Blanca Rosa Caldera. Forms a horst
El San Juan	Reverse fault, dip = 90°	Terminates at: Blanca Rosa Caldera. Forms a horst

3.4.4 Hydrothermal alteration facies model

The hydrothermal alteration facies described in section 2.2.6 were used to build the 3D alteration facies model. The propylitic and potassic facies contain high-temperature alteration minerals; thus, it is essential to interpret their distribution in the reservoir area.

The 3D interpretation of the alteration is modelled and calibrated in this study using the resistivity values corresponding to the low resistivity cap (<15 Ωm) to delimit the bottom part of the smectite layer and obtain a more consistent interpretation of the alteration in the Berlín area. The fault system is not included in the model.

Figure 17 shows the hydrothermal alteration facies. The layers are based on the behaviour and thickness information from the geothermal wells, making the model acceptable. However, in areas where there is no information from wells, the iso-surfaces of the facies have been calibrated based on the resistivity values corresponding to the base of the conductive layer (8-15 Ωm), the top of the layer transition (15-22 Ωm) and the top of the reservoir (30-34 Ωm) for the phyllic, phyllic-propypillic, and propypillic facies, respectively.

Another aspect of the model is that the potassic facie related to the formation of high-temperature minerals (> 250°C) seems to have the shape of a semi-circular contour in the vicinity of well TR-19. Therefore, we propose a relationship between this high-temperature facie and a possible high-temperature source. This relationship with the intrusion model is presented in section 3.4.2. However, as deeper wells are drilled in the area, the limits of this layer could be better adjusted.

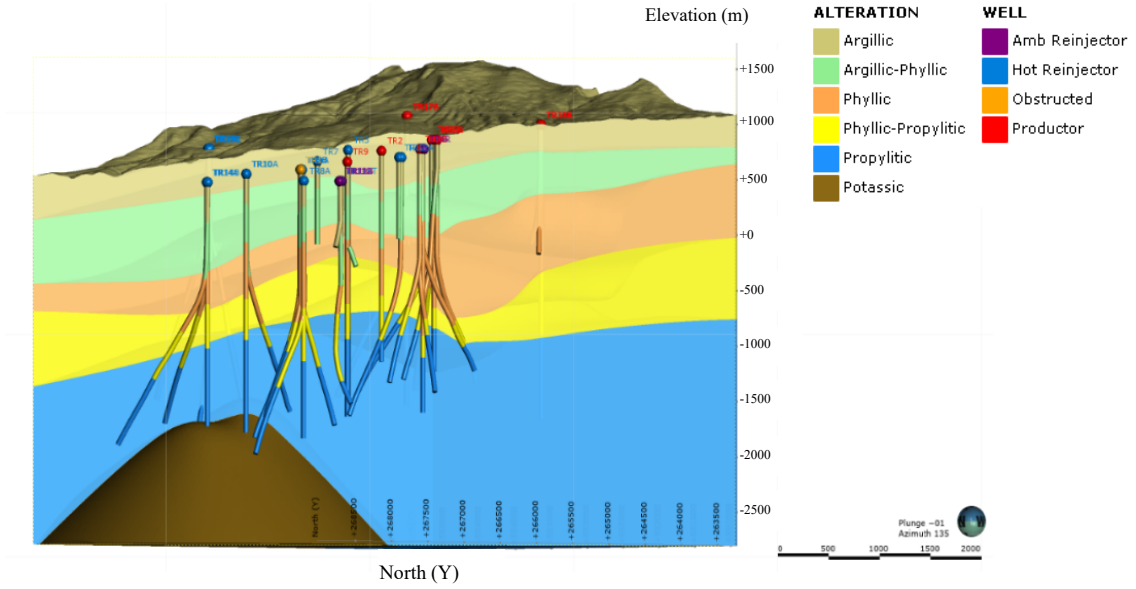

FIGURE 17: Structural system and geological structures in the Berlín geothermal area. The figure legend shows the hydrothermal alteration facies from the wells

3.4.5 Resistivity model

The 3D resistivity model was built using the IDW interpolation model in Leapfrog Geothermal. The format of the original imported file is *.out, and later it was delimited to similar dimensions as the lithological model.

The purpose of generating the electrical resistivity model of Leapfrog Geothermal is to correlate it with different models for the calibration of the facies model and to use it in the weighted model. Therefore, in this section, the model has not been modified; however, cross-sections and some views were created to verify the results obtained using IDW (Inverse Distance Weighted) grid interpolants.

The IDW is a unique way to work with the resistivity data in Leapfrog Geothermal. This is because the IDW interpolants are useful in generating iso-surfaces and volumes from large datasets, such as regular or semi-regular grids. The IDW interpolant interpolates points by taking an average of up to eight nearby samples weighted by their distance (Leapfrog, 2021b).

In the new resistivity model shown in Figure 18, it is possible to observe the resistivity distribution from north to south and east of the geothermal field. The layer with the lowest resistivity (red color; <15 Ωm) is very well defined in the geothermal system. However, it is interrupted as observed to the south where the high resistivity surface (240 Ωm) appears. Likewise, to the north, near well TR-19, another iso-surface of the same resistivity value but of smaller size is observed, suggesting a thermal anomaly zone; however, the temperature values do not reflect this surface.

A cross-section was also built in EW direction using the electrical resistivity values obtained from the 3D model to observe a correlation between the resistivity corresponding to the altered granite (discussed in section 3.4.2) and the hydrothermal alteration facies at great depth (see section 3.4.4).

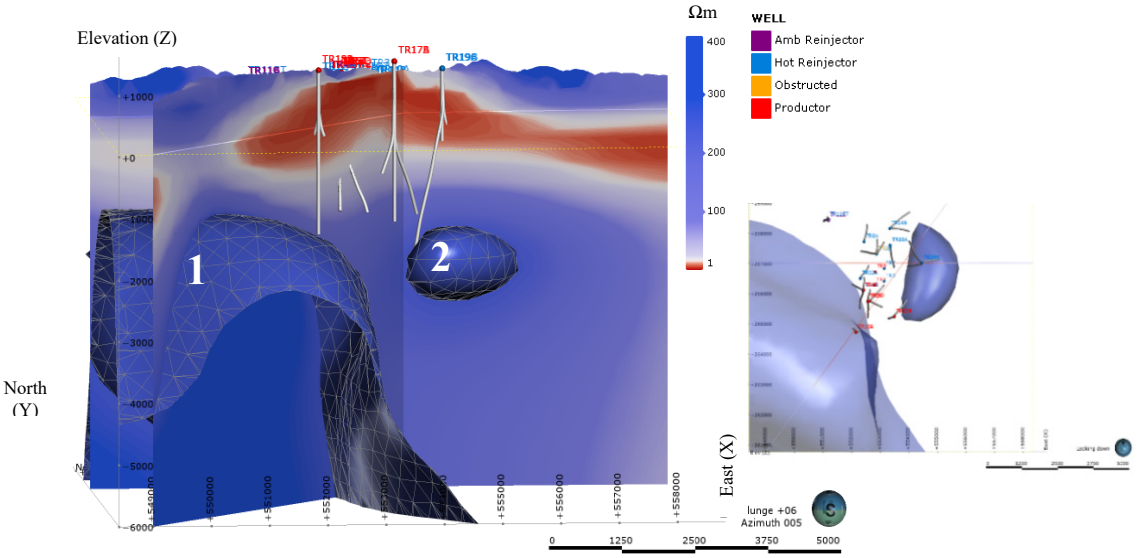

FIGURE 18: Resistivity model using the IDW interpolation model. The model shows the iso-surface of 240 Ωm in two different places (iso-surface 1 and 2). The south area coincides with the presumed heat source (iso-surface 1), and the north area (iso-surface 2), close to reinjection well TR-19, suggests a fossil heat zone (due to the stabilized temperature being low in this zone). The small figure on the right shows the 3D model seen from above

Figure 19 shows that the 160 Ωm iso-surface (blue line) represents the top of the granite (red line) in the northern zone (intercepted by wells TR-14B, TR-19A, TR-19B and TR-19C) and the potassic alteration facie (white line). The above supports the hypothesis that the area where the granite was formed, and high temperature alteration minerals are found, is possibly a heat source zone. The alteration of the rock is due to the effect of temperature and geothermal fluids as indicated by the resistivity values. The rock has probably cooled over time since this does not correspond to values of an intrusive rock without alteration.

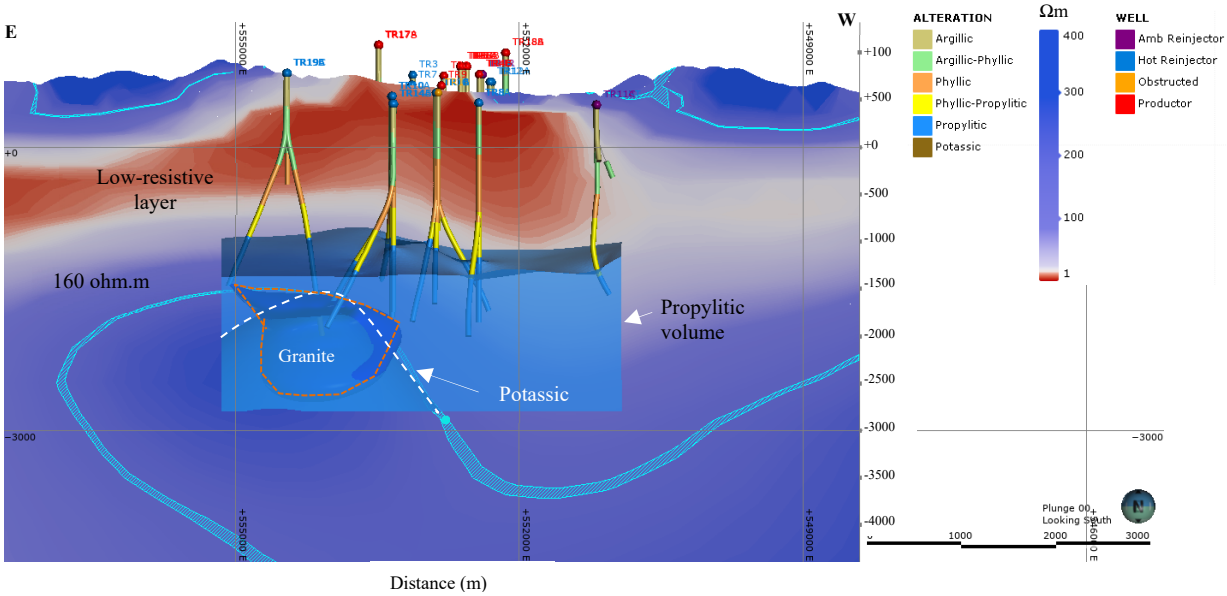

FIGURE 19: Correlation between the hydrothermal alteration facies, resistivity, and the intrusion model

A second correlation model was built to continue the analysis of the resistivity distribution in the geothermal system. Two iso-surfaces of 220-230 Ωm and 250-260 Ωm were used to correlate with the earthquake hypocentres located in 2013-2020 and the gravity map using a density of 2.3 g/cm^3 for Bouguer and terrain correction.

The seismic activity within a geothermal reservoir occurs on fractures and faults of which some are permeable pathways for the circulating geothermal fluid. They are, therefore, a target for geothermal drilling (Hersir et al., 2022). In geothermal systems, the majority of earthquakes occur in the brittle part of the Earth's crust. The brittle-ductile boundary has been identified at 6 km b.s.l. in the Berlín geothermal system according to the seismic hypocenters (Figure 8 in section 2.2.4).

Figure 20 shows the correlation between the results of the three geophysical methods. It is possible to observe that the high gravity anomaly shown on the map (in blue color) correlates with the high resistivity iso-surfaces at great depth, suggesting that it could be the source of the high gravity values. In addition, the seismic activity also indicates that this area could be related to the heat source. The heat source is also hinted at by the brittle-ductile boundary which is at 6 km b.s.l. according to Figure 8. However, in the 3D model, it is difficult to observe the same conductive anomaly, but it could be related to the vicinity of the resistivity iso-surfaces shown in Figure 20, due to a decrease in seismicity.

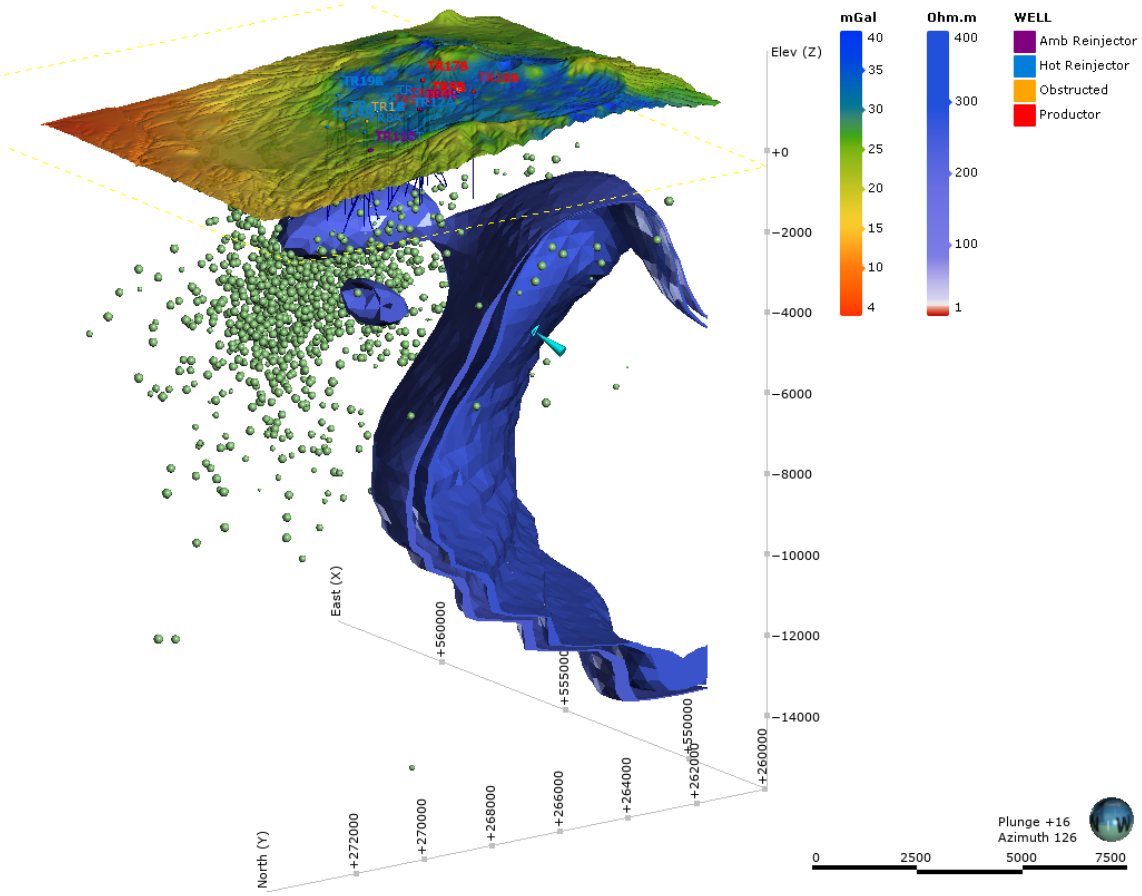

FIGURE 20: Correlation between the iso-surfaces of 220-230 Ωm and 250-260 Ωm, hypocenter distribution (2013-2020) and Bouguer gravity map (LaGeo, 2019)

Of the different data correlations that can be constructed in Leapfrog Geothermal, it is essential to note that data quality, precision, and interpretation of each type of data provide the basis of a reliable

interpretation. Reprocessing of the seismic data and the addition of more MT-TDEM soundings could increase the correlation and therewith the credibility of the data.

3.4.6 Temperature model

The formation temperature model was built using the Radial Basis Functions (RBF) interpolant in Leapfrog Geothermal, which is useful if the data are regularly and adequately sampled, like temperature and pressure well logs.

Before presenting the temperature models, another analysis of the temperature behaviour has been included in this section. The aim is to indicate areas where the temperature has increased or decreased over time and the possible pattern of hot fluid flow in the zone. According to the temperature measured in 2018 in fumaroles, El Tronador (northern area, 98.9°C) and El Hoyón (volcanic area, 96°C) have the highest temperature values; however, to better understand how the temperature changes with time, the temperature differences between 2005 and 2018 have been calculated.

Figures 21-22 shows the fumarole temperature difference between 2005 and 2018. During the last 13 years of monitoring, the temperature has increased in the volcanic and southern areas, possibly due to different reasons: changes in the temperature of the up-flow zone, changes in the pattern of fluid flow, or the proximity of the heat source.

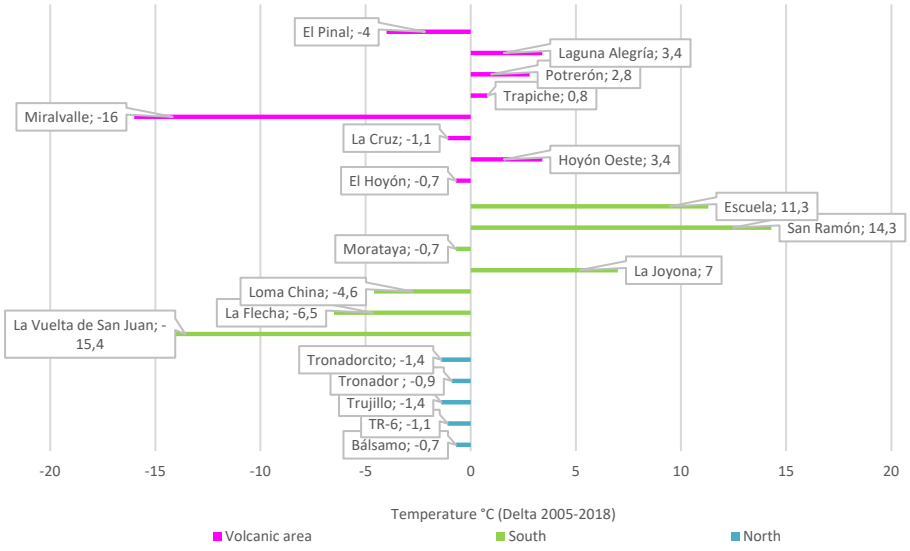

FIGURE 21: Temperature change data of fumaroles located in the volcanic area (pink color), and the southern (green color), and northern (blue color) parts. Data taken from the 2019 conceptual model (LaGeo, 2019)

Thus, it is to be expected that in the temperature model based on the current static PT logs of wells, that the same types of temperature anomalies are seen in these areas.

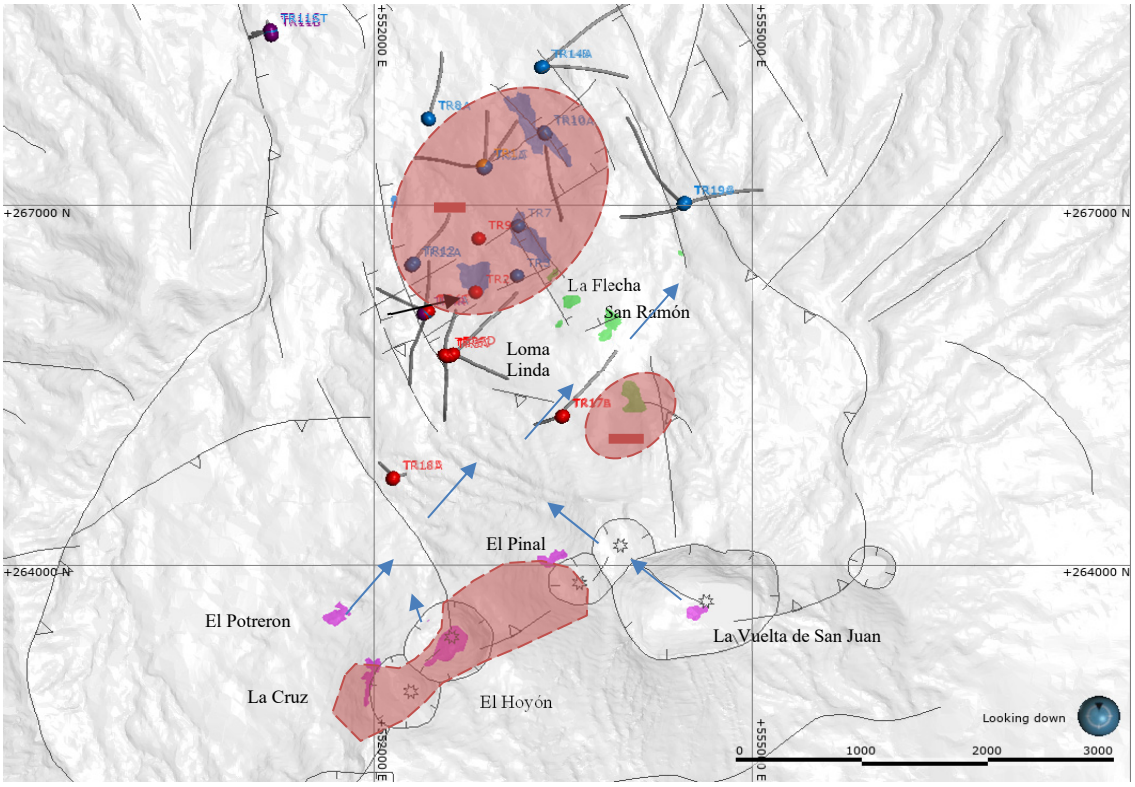

FIGURE 22: Temperature change data from fumaroles locates in the volcanic area (pink color) and southern (green color) and northern (blue color) parts. The red dotted contours show the areas with decreasing temperature and the blue arrows the possible circulation of hot fluid. Data taken from the 2019 conceptual model (LaGeo, 2019)

According to section 2.2.6, the formation temperature distribution at 100 m a.s.l. (see Figure 10) was created using a "Nearest Neighbour" interpolation; however, in this study, the 3D model is created with RBF and New Kriging interpolants to identify differences and validate the new model with the previous model. Also, the importance of this model is to obtain a new 3D model that will be useful to correlate with other geoscientific data, to combine with other models, and include them in the weighted model.

To build the estimation model with the temperature values it is necessary to evaluate the domain estimation that describes the boundary conditions and values used. In this case the selected domain used is the same as for both lithology and alteration facies, with a hard boundary defined. Figure 23 shows only the data used within the domain's boundary (all temperature data inside the hard boundary). This means that the values used do not extend beyond the boundary.

After the data analysis and domaining, the next step is the construction of the variogram, which can be used for different types of interpolants. In this study, Kriging is the interpolant used with this methodology that will be compared to the RBF interpolant model and the initial temperature model.

In general terms, the variogram is the analysis of spatial variability of grade within a region. In this case, the temperature values have a relatively low spatial variability between samples. Figure 24 shows the Sill parameters, which define the upper limit of the model and the distance where no correlation between values exists.

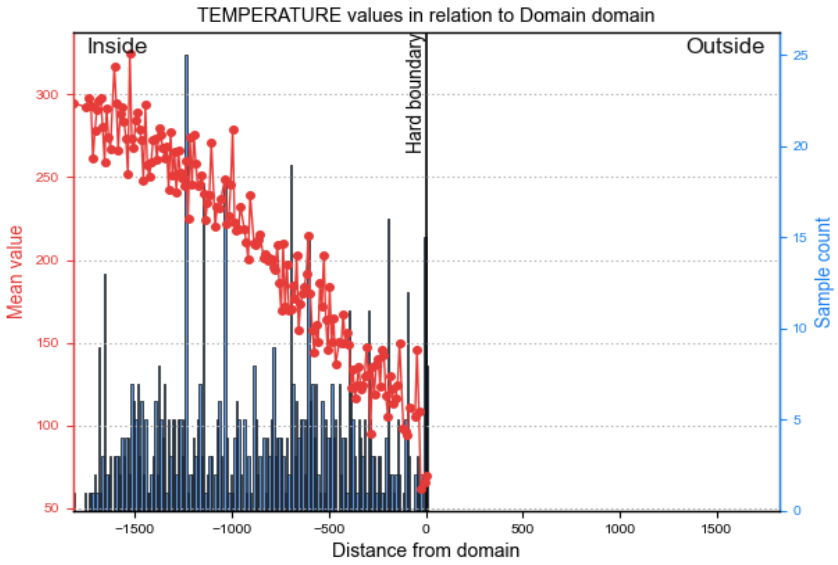

FIGURE 23: Graph of the temperature values in relation to the domain used (Statical graph from Leapfrog Geothermal)

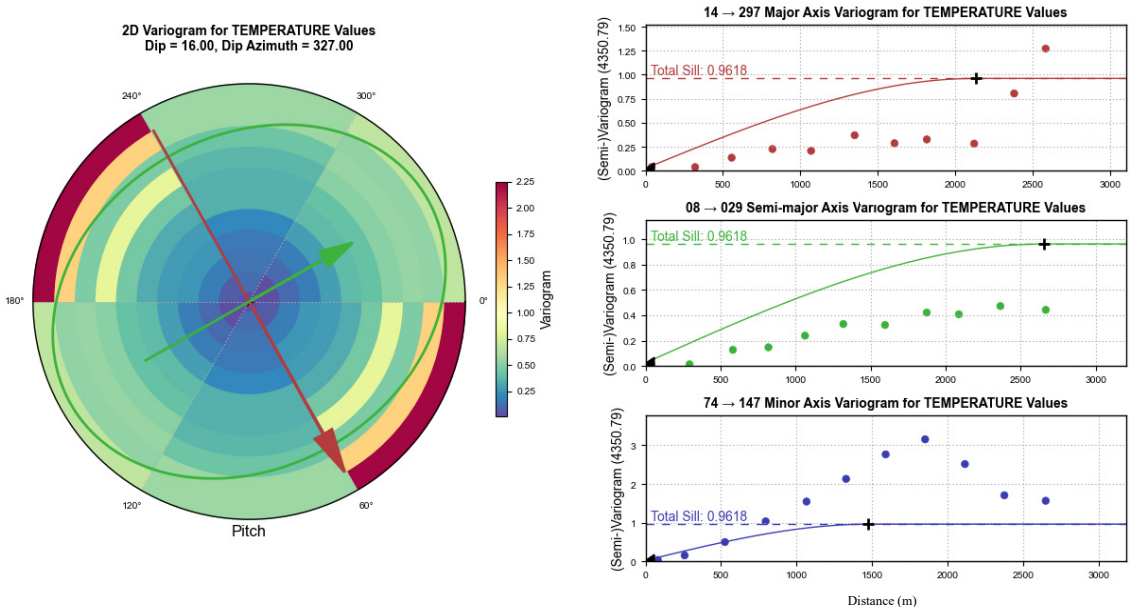

FIGURE 24: 2D variogram for the formation temperature values and the different Sill axis manipulated for the final model

When comparing the model built with Kriging interpolation with the initial model with (NN) Nearest Neighbour interpolation, no significant differences are observed, which indicates that the parameters used for the temperature data have been well selected. Figure 25 shows that the highest formation temperatures are concentrated in the southern zone and the centre of the geothermal field in both interpolations.

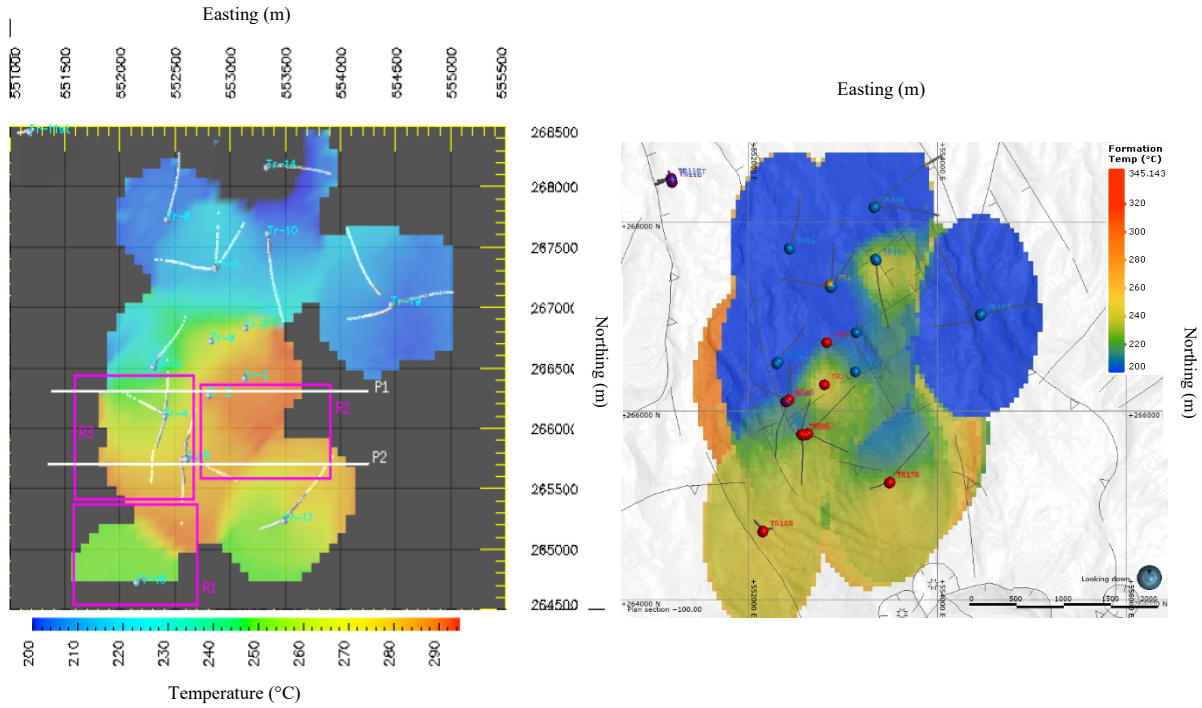

FIGURE 25: Comparison of temperatures between the reference temperature map and the new model using different types of interpolation at the same elevation (100 m a.s.l.). Model a) was built using "Nearest Neighbour" interpolation and b) was built using Kriging interpolation

Likewise, the stabilized temperature model and the temperatures obtained from the last PT records in each well were built to obtain a model with the difference of temperature data that indicates the areas where the temperature has increased significantly, in addition to including the latest PT records in the weighted model. Figure 26 shows the temperature models used for the temperature change model (ΔTemperature model, Figure 27).

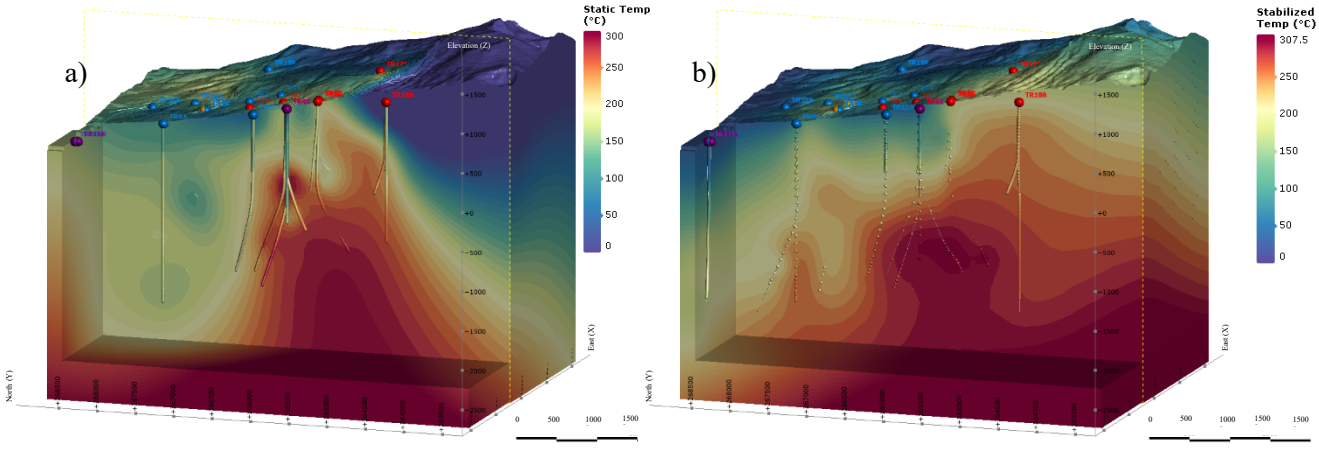

FIGURE 26: Comparison between a) the stabilized profile (first 5 years after drilling) and b) static temperature (2018-2021) profile from the geothermal wells. The most recent model shows significant changes in the temperature from the center to the areas in the north

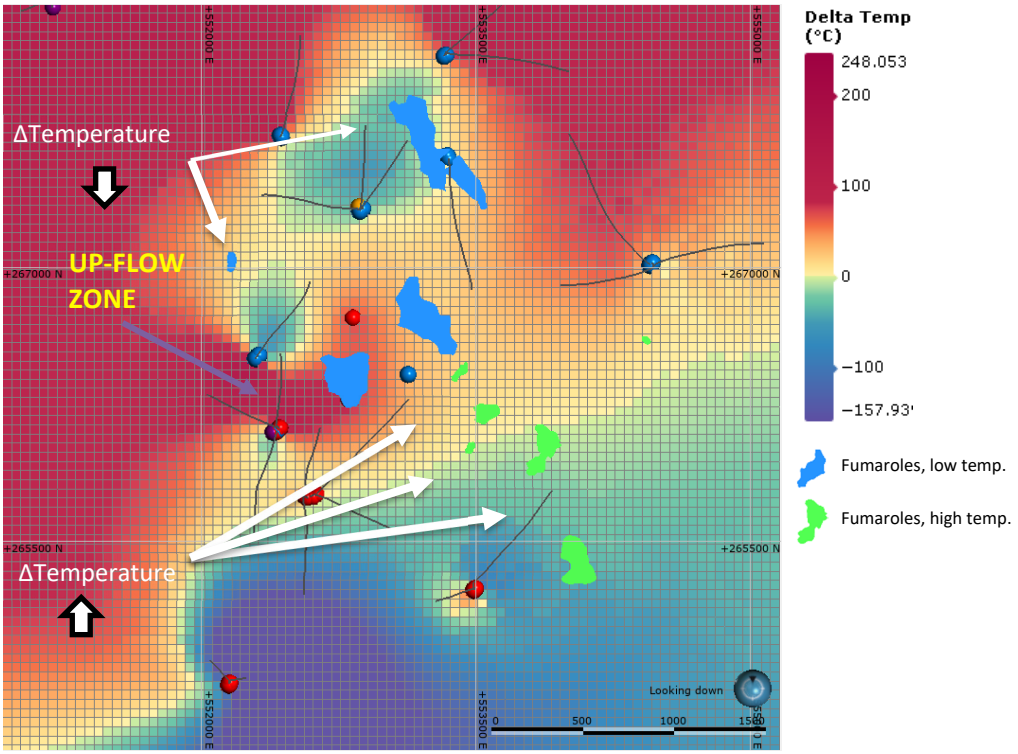

FIGURE 27: Temperature change (ΔTemperature) model (static temperature-stabilized temperature). The model shows the temperature at 325 m a.s.l., indicating the elevation where there is similar change in temperature measured in fumaroles (see Figure 18)

3.4.7 3D Feed zone model

The steam cap of the geothermal field has been identified in production wells TR-18A and TR-18B. The steam flow rates of TR-18A and TR-18B are 41 kg/s and ~ 10 kg/s, respectively. Therefore, identifying the possible boundaries of the steam cap is of interest for this work.

The 3D feed zone model is a test model of the possible boundaries of the fluid pattern, considering the main feed zone of each production well as the most significant fluid contributor. The created 3D mesh connects each point so that it is possible to observe the fluid movement pattern, which is considered two-phase in this model.

In general terms, Figure 28 shows how the circulation pattern of fluids in the feed zone mesh is possibly influenced by the fault system. Another important aspect to observe is how the main flow from the southern part circulates in the direction of well TR-1 at similar depths and changes at the Old Berlín Caldera barrier, indicating that the fault system controls the fluid pattern. An evaluation of the resistivity model indicates that the southern and central zones intersect part of the cap-rock (6-10 Ωm) of the system while resistivity values to the NE and N correspond to the reservoir top (>25 Ωm), indicating that the fault system possibly influences the system. Likewise, Table 4 shows the temperature values evaluated in the model.

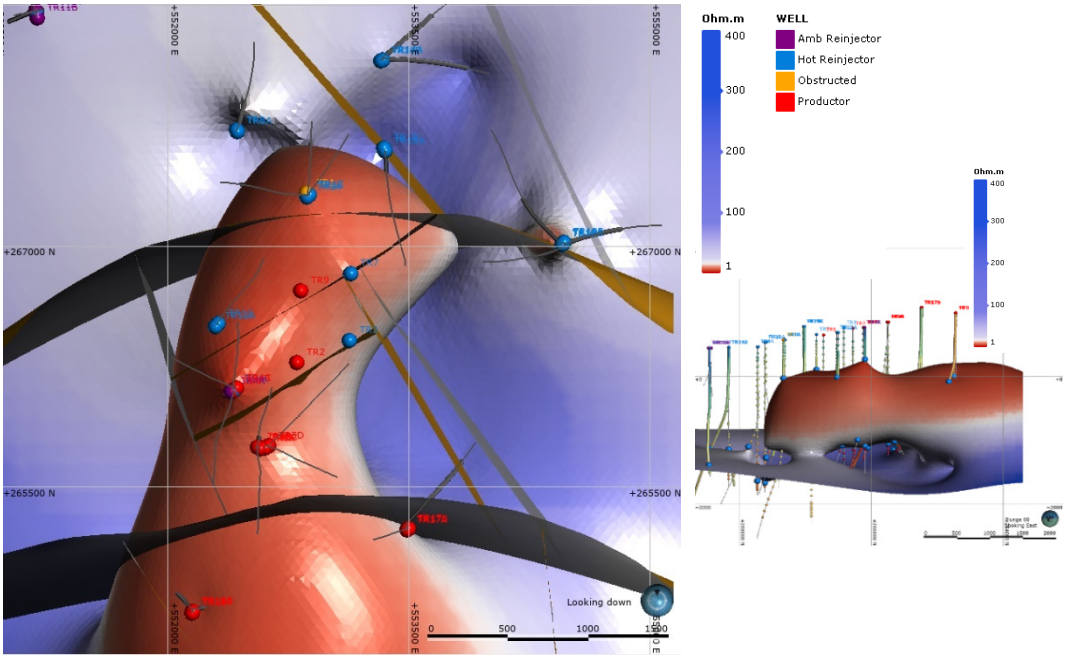

FIGURE 28: Feed zone mesh evaluated from the 3D resistivity model. The small figure to the right shows the 3D model from above. The model interacts with the main fault system and indicates a probable fluid pattern.

TABLE 4: Maximum steam flow rate in the production wells, in 2020-2021 (LaGeo, 2021b)

Well	Steam flow rate (kg/s)	X	Stabilized temperature in the feed zone (°C)	Formation temperature in the feed zone (°C)	Depth to the feed zone (MD)
TR-2	15.5	0.25	298	298	1750
TR-4B	11.6	0.26	290	294	1800
TR-4C	8.6	0.25	277	277	1900
TR-5	19	0.22	305	302	1900
TR-5A	15.5	0.21	298	--	2100
TR-5B	16	0.22	292	286	2000
TR-5C	14.8	0.23	302	293	2000
TR-5D	14	0.17	278	--	1825
TR-9	7.1	0.19	296	290	1800
TR-17	15.9	0.21	248	247	1350
TR-17A	8.7	0.16	240	271	2350
TR-17B	18	0.23	257	250	1650
TR-18	17.5	0.20	263	263	2400
TR-18A	41	1.0	240	--	1000
TR-18B	8.7	1.0	242	--	1100

Continuing with the same analysis and considering the same main feed zone for all geothermal wells, another model was built with a different interpolation. In this case a 2D interpolating mesh was used that connects each feed zone at the exact depth to avoid building a closed mesh like a volume shape shown in Figure 28. This new mesh model shows a clear connection between the different locations of the feed zones and their interception with the faults. The most significant changes in the face dip of the model correspond to the significant changes in the location of the feeding zone in a small area that also

has a high interconnection with the fault systems. Figure 29 shows the new mesh that interconnect the feed zone point of all geothermal wells.

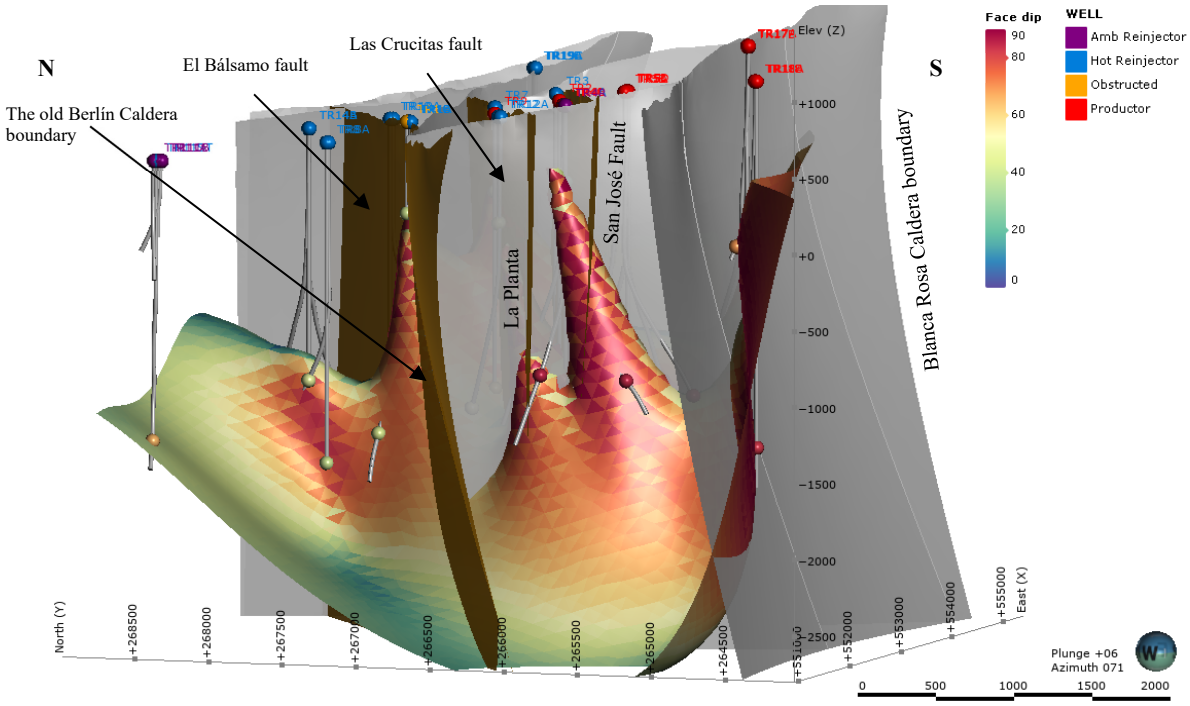

FIGURE 29: Feed zone mesh constructed using 2D interpolating mesh in Leapfrog Geothermal

3.4.8 Combined models

An important part of the modelling process is combining results for a better understanding and visualization of the various anomalies and their possible causes. The combined model permits to delineate anomalies in one dataset and comparisons with other datasets become easier.

In this work, different parameters from previous models described in the sections above have been combined. The combination models are listed below:

a) Resistivity and temperature models

The stabilized temperature and resistivity models were correlated through a combined model using specific parameters representing the top of the geothermal reservoir. Figure 30 shows the resistivity values from 30 to 50 Ωm and temperatures values >260°C together with several structural faults of the system that are suggested to be the primary limits of the top of the reservoir. To the north, the Old Berlín Caldera represents the limit at 1,100 m b.s.l., to the east it is limited by the El Tronador fault at 600 m b.s.l., and to the west at 1,200 m b.s.l. the reservoir is probably limited by the extension of the El Hoyón fault. It is interesting to observe the results because they give a general idea of the behaviour of the top of the reservoir according to resistivity and stabilized temperature.

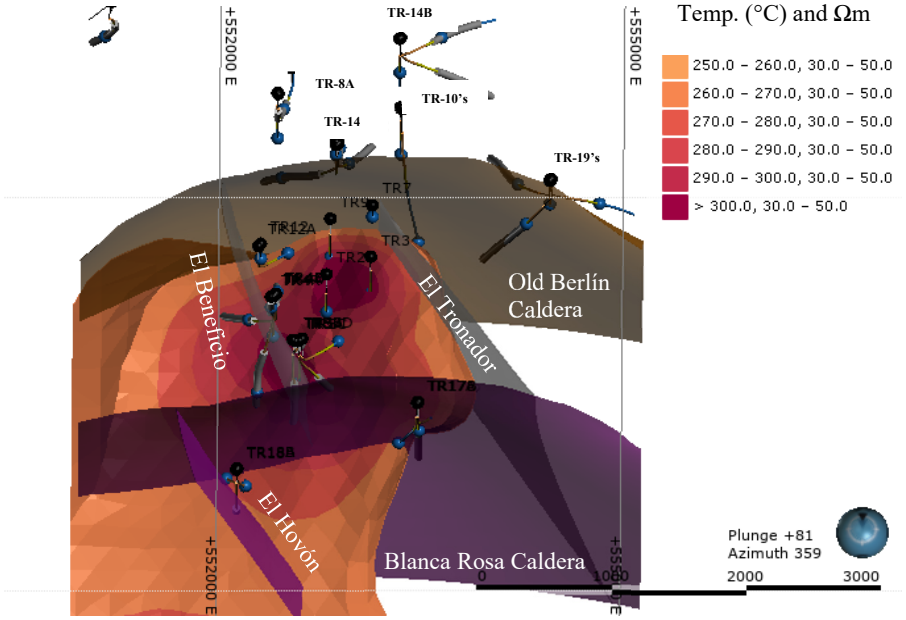

FIGURE 30: The combined model for Berlín of resistivity and temperature constrained by several structural faults that might represent the limits of the top of the geothermal reservoir

b) Stabilized temperature and pressure model

Only the temperature and pressure values identified in wells TR-18A and TR-18B, corresponding to the main feed zones, have been discretely selected to construct the combined model (see Figure 31). The ranges of values considered for temperature and pressure are 230-270°C and 30-40 bar g, respectively. These wells were selected because they intercept the steam cap of the geothermal system.

The model suggests a possible volume extension from the south, where the thickness is high, towards the north (close to well TR-5, TR-4, and TR-2) and southeast zone (close well TR-17).

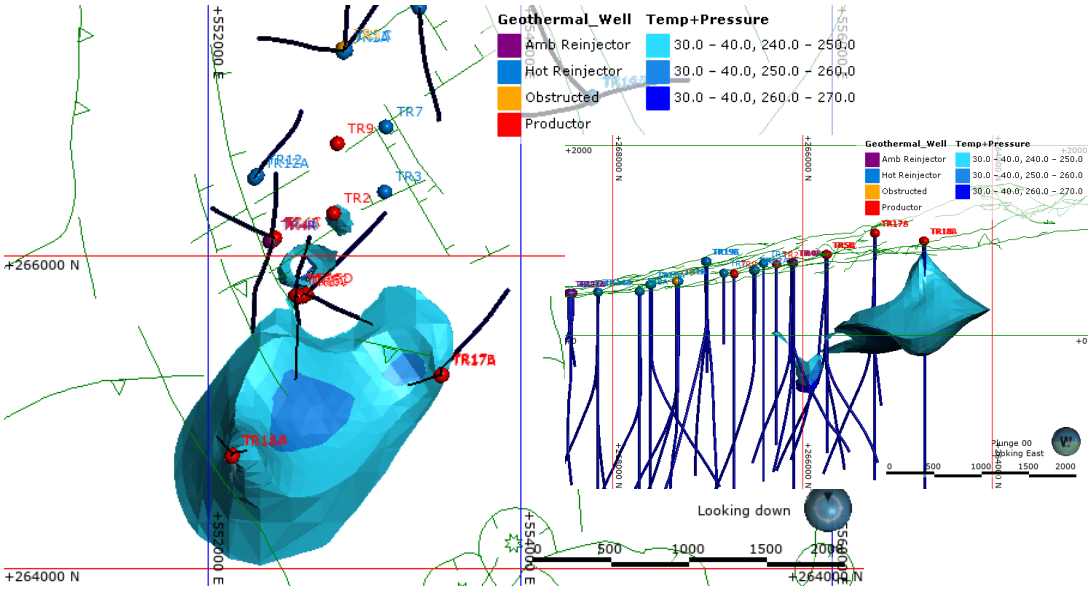

FIGURE 31: The combined stabilized temperature and pressure model for Berlín shows the volume with temperatures around 230-270°C and pressure between 30-40 bar g

The second volume identified in the zone of well TR-2 is caused by the interpolation effect due to the high-temperature values in TR-1A (230°C at 1,400 m depth). Therefore, it is omitted in this analysis.

For a better estimation and further analysis, it is suggested that future studies include the deep geochemistry of the production wells and evaluate the model with recent PT logs because the thermodynamic properties of the steam cap can change and evolve over time.

3.4.9 Weighted model and quantification of favourable drilling targets of the area

The integration of multiple data sets enables advanced processing and calculations similar to Play Fairway Analysis (PFA), a methodology adapted from the oil industry that integrates data at the regional or basin-scale to systematically define favourable plays for the exploration (Shervais et al., 2020). In this work, the favourable model is a weighted model where the weighting value for each model is defined according to parameters or characteristics that best describe the geothermal reservoir. After the characterization of the reservoir, calculations are made to obtain favourable areas that represent the best drilling targets. Figure 30 shows the weighting values applied to the models included in the weighted model.

The block model size of the evaluations and calculations is shown in Figure 32; the dimensions applied are 50 m for the X, Y, and Z axes.

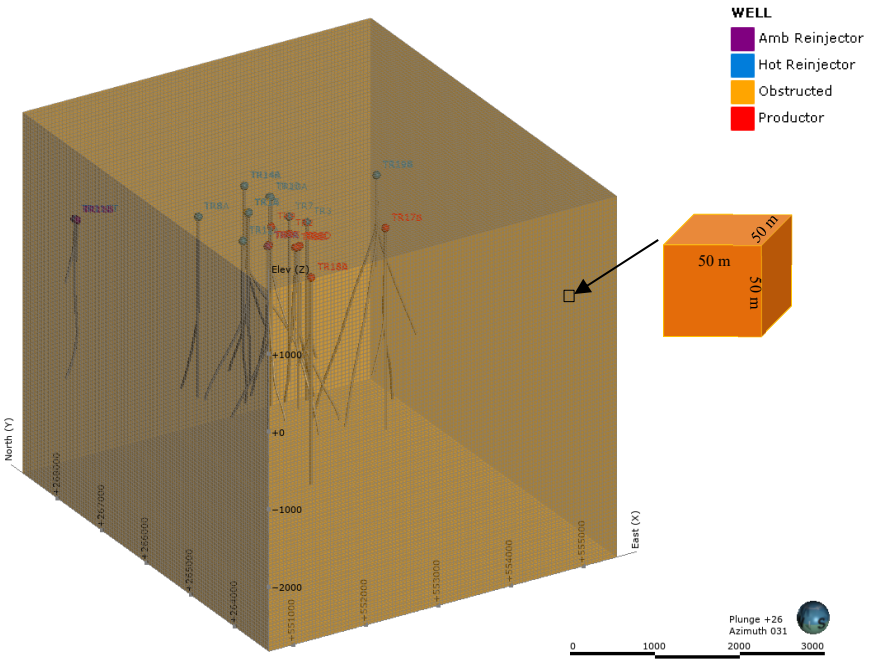

FIGURE 32: Block model size used for the evaluations of 3D models and building the weighted model. The orange cube indicates the size for each cube in the block model

After creating the block model, the next step is to identify the priority levels for each model evaluated and discussed in previous sections. The priority levels range from 0 to 6. Number five and six are the most relevant in the weighted model, representing the characteristics of the area of the potential geothermal reservoir. Equations (2) to (9) show the levels applied for each model.

```
Lithology_Index = if
    [Lithology Units_Modified_WithCalderas] = 'UI'   → 1
    [Lithology Units_Modified_WithCalderas]= 'UII'   → 2
    [Lithology Units_Modified_WithCalderas]= 'UIII'  → 3
    [Lithology Units_Modified_WithCalderas]= 'UIV'   → 5
    otherwise                                        → 0
```

(2)

```
Facies_Index = if
    [Alteration Facies_Calibrated Rest]= 'Argillic'             → 1
    [Alteration Facies_Calibrated Rest]= 'Argillic-Phyllic'     → 2
    [Alteration Facies_Calibrated Rest]= 'Phyllic'              → 3
    [Alteration Facies_Calibrated Rest]= 'Phyllic-Propylitic'   → 3
    [Alteration Facies_Calibrated Rest]= 'Propylitic'           → 5
    [Alteration Facies_Calibrated Rest]= 'Potassic'             → 5
    otherwise                                                   → 0
```

(3)

```
Distance to Faults_... = if
    0 <= [Distance to Faults] <100   → 4
    100 <= [Distance to Faults] <150 → 3
    150 <= [Distance to Faults] <200 → 2
    200 <= [Distance to Faults] <250 → 1
    250 <= [Distance to Faults] <300 → 1
    otherwise                        → 0
```

(4)

```
Stabilized Tempera... = if
    0 <= [Stabilized Temperature] <75    → 0
    75 <= [Stabilized Temperature] <125  → 1
    125 <= [Stabilized Temperature] <175 → 2
    175 <= [Stabilized Temperature] <225 → 3
    225 < [Stabilized Temperature] <240  → 4
    240 <= [Stabilized Temperature] <260 → 5
    260 <= [Stabilized Temperature] <300 → 5
    otherwise                            → 6
```

(5)

Formation temper... = if

0 <= [Kriging, Formation Temperature] <75	→ 0
75 <= [Kriging, Formation Temperature] < 125	→ 1
125 <= [Kriging, Formation Temperature] <175	→ 2
175 <= [Kriging, Formation Temperature] <225	→ 3
225 < [Kriging, Formation Temperature] <240	→ 4
240 <= [Kriging, Formation Temperature] <260	→ 4
260 <= [Kriging, Formation Temperature] <300	→ 4
otherwise	→ 5

(6)

Resistivity_Index = if

0 <= [BLN_1903_06_3dmod_last] <10	→ 3
10 <= [BLN_1903_06_3dmod_last] <30	→ 4
30 <= [BLN_1903_06_3dmod_last] <45	→ 5
45 <= [BLN_1903_06_3dmod_last] <100	→ 5
100 <= [BLN_1903_06_3dmod_last] <200	→ 4
otherwise	→ 0

(7)

Distance to drilled ... = if

0 <= [Distance to drilled wells] <300	→ 0
300 <= [Distance to drilled wells] <500	→ 4
otherwise	→ 5

(8)

Distance to feed_z... = if

0 <= [Distance to well_feedzone] <200	→ 2
200 <= [Distance to well_feedzone] <300	→ 3
300 <= [Distance to well_feedzone] <400	→ 5
otherwise	→ 6

(9)

Figure 33 shows schematically how the weighted model was constructed together with the weight values for each model. Equations (10) to (14) show the different evaluations and weights for each model, starting from a simple model (Equation 10) to a more complex one (Equation 14).

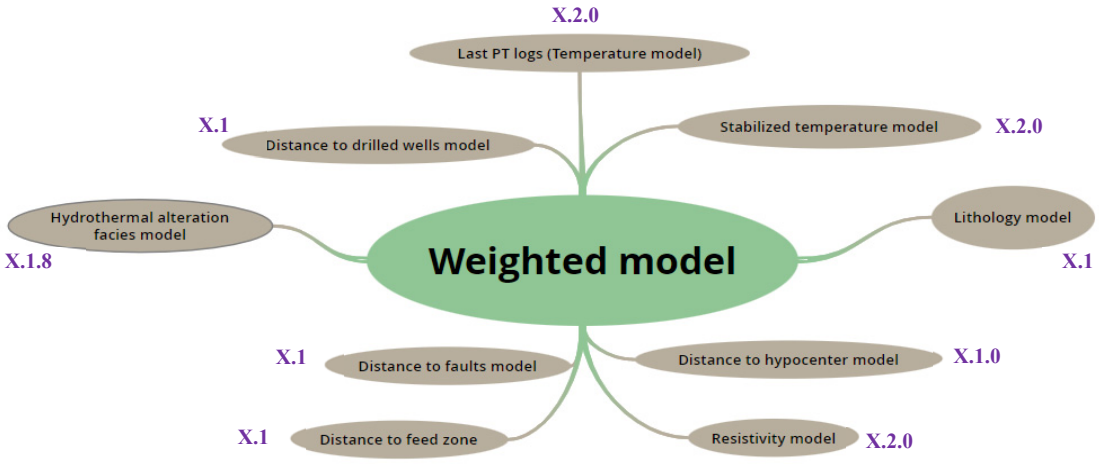

FIGURE 33: Weight values applied to the models included in the weighted model in Leapfrog Geothermal

Weighted model 1

$$= (1 * [Lithology\_Index] + 1.8 * [Facies\_Index] + 2 * [Stabilized\ Temperature\_Index] + 2 * [Resistivity\_Index])/3.5 \quad (10)$$

Weighted model 2

$$= (1 * [Lithology\_Index] + 1.8 * [Facies\_Index] + 2 * [Stabilized\ Temperature\_Index] + 1.5 * [Distance\ to\ Seismicity\_Index] + 2 * [Resistivity\_Index])/4.15 \quad (11)$$

Weighted model 3

$$= (1 * [Lithology\_Index] + 1.8 * [Facies\_Index] + 2 * [Stabilized\ Temperature\_Index] + 1.5 * [Distance\ to\ Seismicity\_Index] + 2 * [Resistivity\_Index] + 1 * [Distance\ to\ Faults\_Index])/4.55 \quad (12)$$

Weighted model 4

$$= (1 * [Lithology\_Index] + 1.8 * [Facies\_Index] + 2 * [Stabilized\ Temperature\_Index] + [Distance\ to\ Seismicity\_Index] + 2 * [Resistivity\_Index] + [Distance\ to\ feed\_zones] + [Distance\ to\ drilled\ wells\_Index])/4.85 \quad (13)$$

Weighted model 5

$$= (1 * [\text{Lithology\_Index}] + 1.8 * [\text{Facies\_Index}] + 2 * [\text{Stabilized Temperature\_Index}] + 1 * [\text{Distance to Seismicity\_Index}] + 2 * [\text{Resistivity\_Index}] + [\text{Distance to Faults\_Index}] + [\text{Distance to feed\_zones}] + [\text{Distance to drilled wells\_Index}])/5.4 \quad (14)$$

Figures 34 to 36 show the evolution and comparison for each calculation applied in Equations (10) to (14). The differences correspond to the weighting value and the models. Thus, each figure explains briefly the considerations for each weighted model.

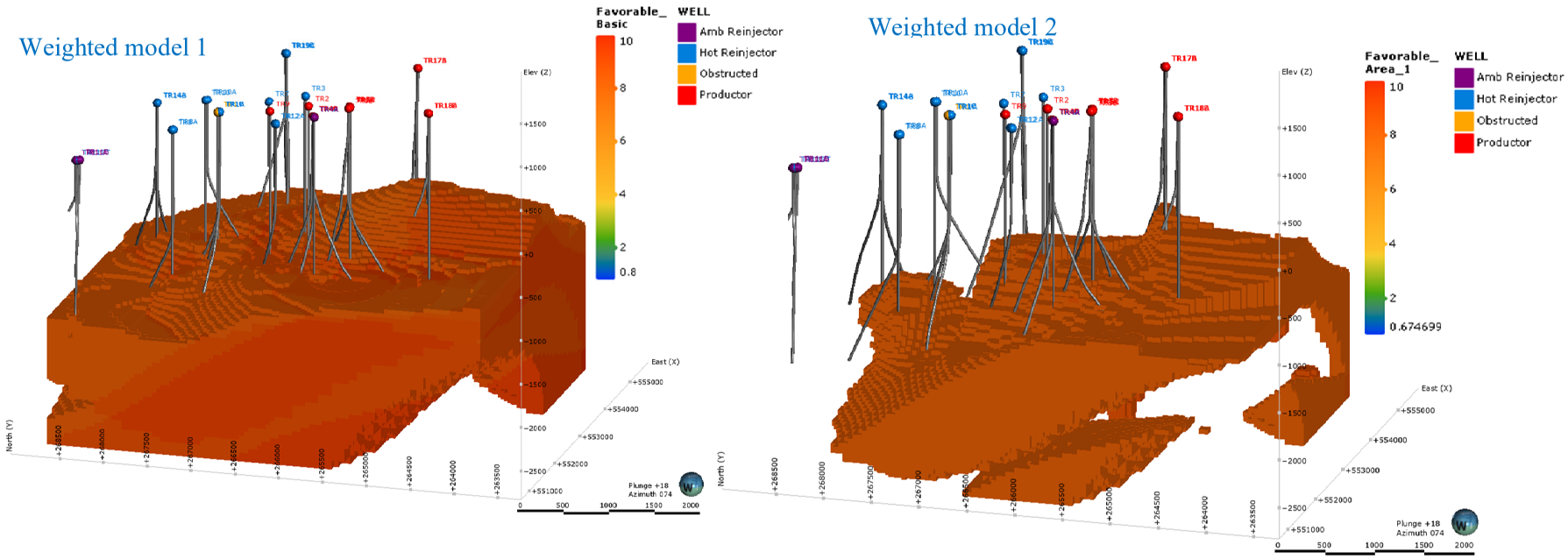

FIGURE 34: Comparison of the weighted models 1 and 2 for Berlín. The first model is a basic model where most of the data corresponding to information from wells, and the weighted model 2 is more complex adding the "distance to the hypocenter" seismic model. Both models show the favorability area between 80 to 100%

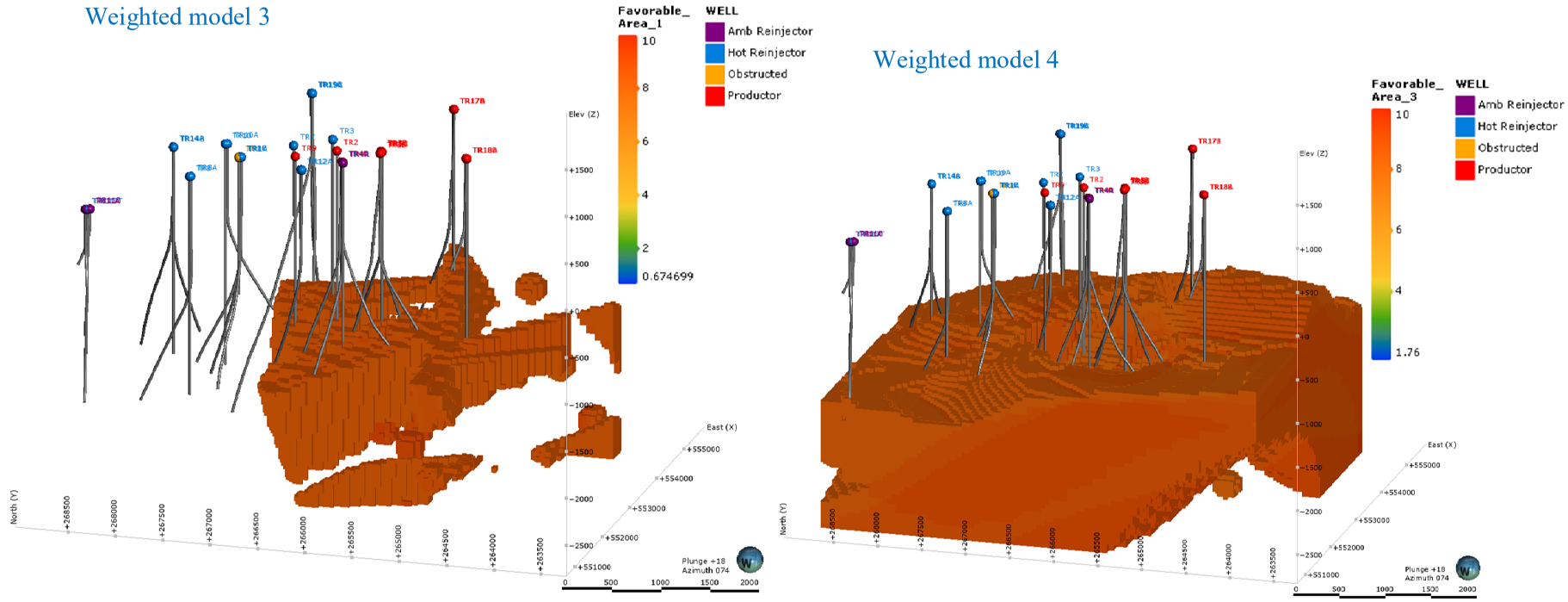

FIGURE 35: Comparison of weighted models 3 and 4 for Berlín. The third model is a more discrete model with the inclusion of the fault system with a greater weight than the fourth model, reducing the favourable area. In contrast, the fourth model shows a larger area of favorability because the additional well information has the same weight. Both models show the favorability area between 80 to 100%

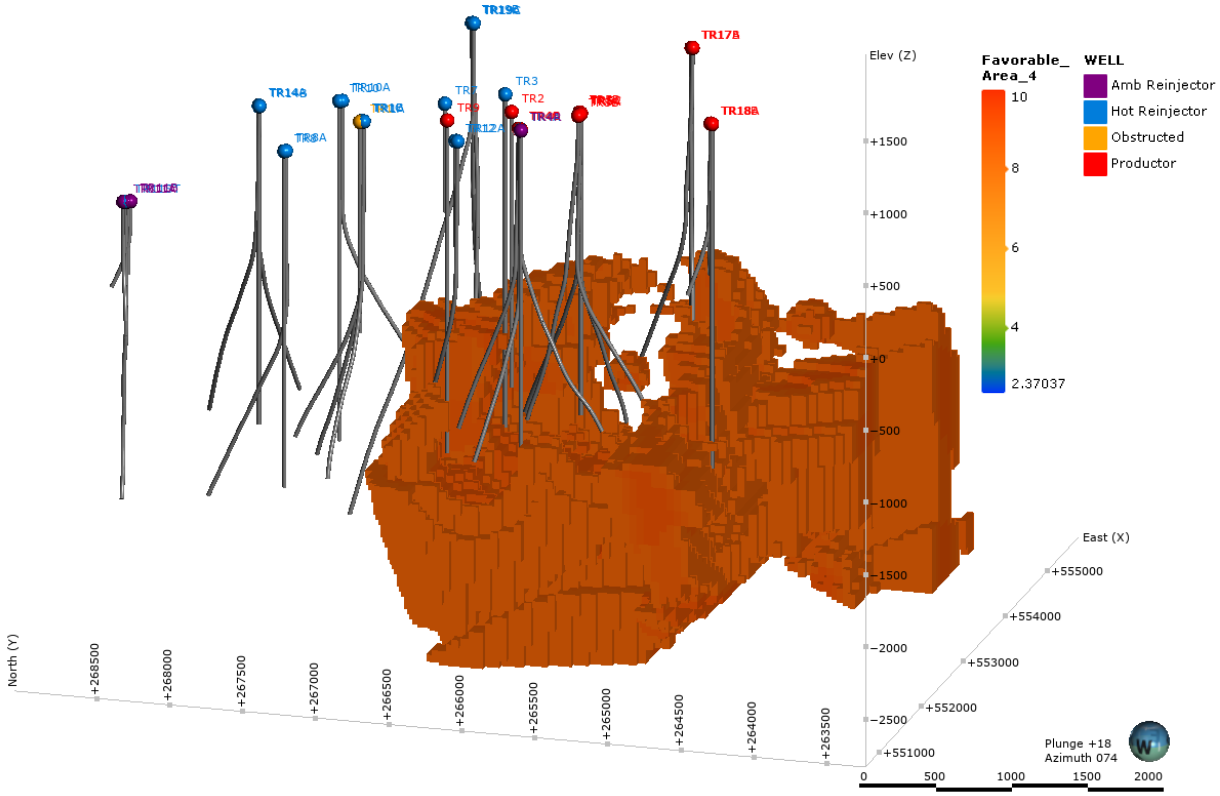

FIGURE 36: Weighted model 5 for the Berlín geothermal system. The model is the result of the calculation performed by Equation (14). The weighted model includes 3D models (discussed in the Results section). The weighted model shows areas for drilling targets with >85% favorability

For better visualization of the new weighted model for the Berlín geothermal system, Figure 37 shows a map view in which different areas of interest are represented that could be considered as drilling targets areas for new production wells (8.5-10). There are two groups of favourable areas: the first group (1, 2, 3, 4 and 5) are the primary zones, represented by green squares where the extrapolation is less than in other model areas, and areas 6, 7 and 8 are the secondary areas that are represented by blue squares. The secondary areas have higher uncertainty because here the model has been extrapolated to a greater extent. This could, however, be verified with results from new wells.

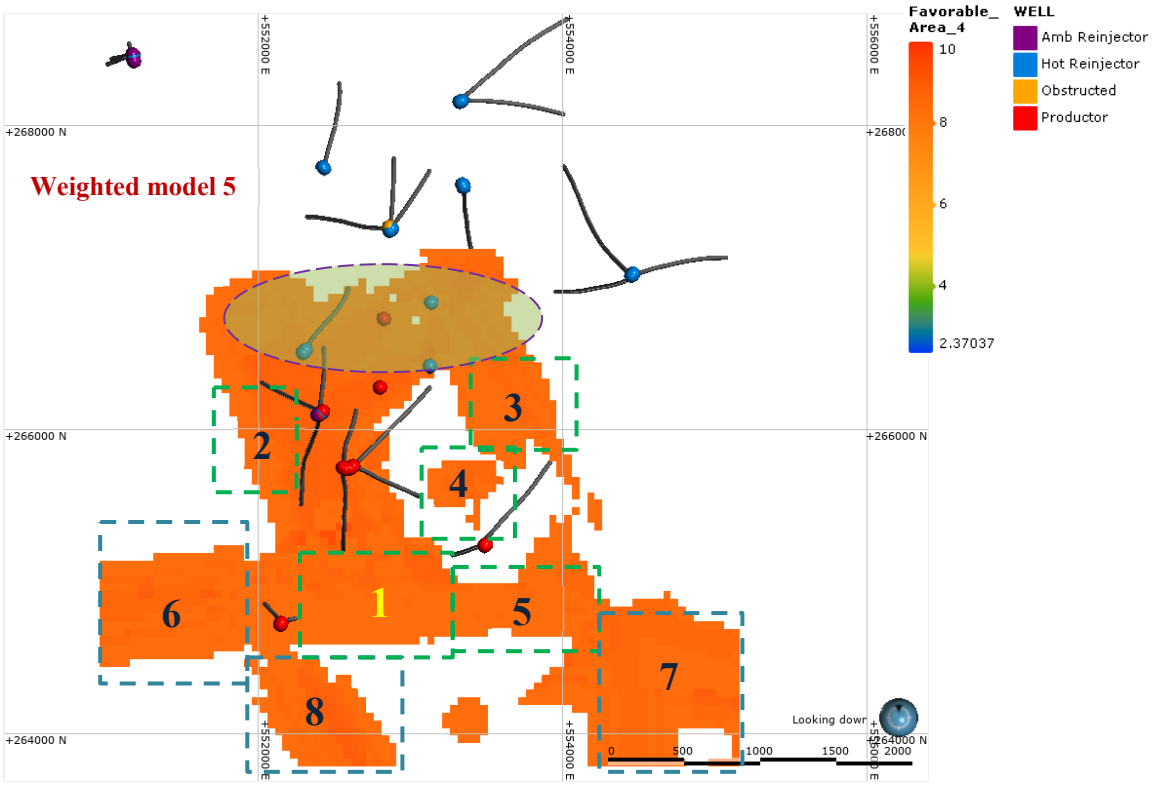

FIGURE 37: The 3D weighted model seen from above. The most favourable areas are inside the green boxes (area: 1, 2, 3, 4 and 5) and the exploratory areas or secondary areas due to extrapolation in the model are inside the blue boxes (area: 6, 7 and 8). Area 1 represents the most favourable area for siting the next production wells according to the combined model (pressure + temperature models). The models show the favorability area between 85 to 100%

Another important aspect of the weighted model is observed in reinjection wells TR-12, TR-3, and TR-7, which are also favourable areas for drilling new producing wells. This is because the location of the reinjection wells has not been considered in the model; however, it is interesting to note that there is a high probability of finding a good geothermal resource in this area but at greater depths. The reinjection wells drilled in this area do not reach depths greater than 2,400 m, therefore, they do not intercept the depth-range of the model.

4. DISCUSSION

For the first part of this study, all available geoscientific data were gathered, digitized, and standardized in terms of units and formats. The available data were used to revisit the conceptual model of the Berlín geothermal system to construct a three-dimensional (3D) model of each type of data or information and construct a weighted model that indicates the most favourable drilling targets by assigning values from 0 to 10 (see the colour scale in the weighted models); however, the results in this project are limited to areas which were assigned ratings from 8 to 10 because they represent the volumes where the most important parameters of each model are favourable and converging (Equations 2, 3, 4, 5, 6, 7, 8 and 9). The 3D models were created in the Leapfrog Geothermal 3D modelling tool; however, chemical data and alteration minerals from wells have not been included in the weighted model due to lack of time to rearrange the information into the format required by the software.

The 3D lithology model was built using information from cores of the wells (information validated and analysed by geologists from LaGeo, 2019). The model interacts with the main fault systems of the area (NW-SE and NE-SW system and the two caldera boundaries). It suggests block motions according to the fault type (normal or reverse); therefore, they were analysed according to the depth of the four rocks units (I, II, III, and IV). The movements of the blocks of rock proved to be consistent with the lithology information and known intersection with feed zones. Therefore, the model suggests that some faults, primarily the Calderas boundaries, have affected the rock deposits and that the caldera structure plays an important role in the fluid flow and its connection with the fluid flow patterns in this area. This is consistent with the connections between the production and reinjection wells. The earlier data presentation included dip and azimuth values of the faults. Now, the lithological 3D model is in digital form, which will benefit future modelling work in the area.

The 3D hydrothermal alteration facies were modelled to show the trend of the alteration facies and the related high-temperature environment (based on the temperature required for mineral formation). The model was calibrated by the resistivity data and compared to current and stabilized temperatures. The results show a sealing layer (argillic-phyllic facie) beginning at 860 m b.s.l. in the southern part indicating a stabilized temperature range of 178-235°C. The temperature in the neighbouring wells TR-17 and TR-18 is currently around 185-247°C, indicating an increase of temperature in the southern area. However, a decrease in temperature has been identified in the northern zone, specifically in wells TR-8, TR-14, and TR-19, observing a decrease of ~ 30°C on the first two platforms and ~ 19°C on the TR-19 platform. With this hydrothermal alteration facies, detailed data of alteration minerals could be added to the model to generate a more reliable model of the lithology to be related to different temperature models.

A 3D feed zone model was constructed using the main feed zone of each geothermal well to infer the trend of geothermal fluid flow in the area. In addition, the model was calibrated comparing the temperature and pressure data to different parameters ensuring a better reliability of the model. The mesh covers all geothermal wells (production and reinjection wells). It can be observed that between 500 m and 1,100 m depth the superficial fluids are confined in the northern part by the old Berlín Caldera. This implies that the fluids are possibly reaching to greater depth in the north. The current pressure evaluated in the mesh is around 33 bar g in well TR-18, where the steam cap has been identified, and similar values are found in well TR-17. However, in the wells located in the central and northern areas, the pressure increases and the temperature decreases, possibly due to reinjection. High-temperature values have been identified close to wells TR-5 and TR-4, which support the notion of a possible up-flow zone in the central area. In addition, the evaluation of the resistivity model indicates that the southern and central zones intersect part of the cap rock (6-10 Ωm) of the system.

The correlation between the resistivity and temperature models has demonstrated that it is possible to build relationships representing the geothermal reservoir. Therefore, its possible extension can be characterized according to the resistivity and temperature ranges. Resistivity values from 30 to 50 Ωm and temperatures values >260°C correlate with structural faults of the system, which appear to be the primary limits on the top of the reservoir. The model could be a good input for updating the resource production strategy when new information is obtained from well PT profiles, or the resistivity model is updated.

Finally, the correlation in the weighted model based on the different 3D models gives a good visualization and representation of the geothermal system. The use of the Edge extension in Leapfrog Geothermal has permitted modelling and rating of the most favourable drilling target areas in a range from 1-10 (or 10-100%). From the five weighted models, model number 5 is the best because it considers as many models and data as possible to decrease the uncertainty. There are five favourability areas with values >85% and high certainty and an additional three areas with values >85% and low certainty due to extrapolation. However, the weighted model could represent an excellent input and tool to explore new drilling target areas. In addition, the update and calibration with new well(s) or more detailed information could help improve the weighted model.

5. CONCLUSIONS AND RECOMMENDATIONS

5.1 Conclusions

The Berlín geothermal field has been utilized since 1992 when the first two back pressure units were installed as a pilot project. As the area was explored and harnessed over the past 29 years (1992-2021), a significant number of reports have been published including six reports involving updates of the conceptual model of the Berlín geothermal field. This has made it possible to identify and propose new drilling targets for production and reinjection wells.

One of the main objectives of this project was to generate and suggest a workflow for the construction of different types of models of the geothermal area that are the main inputs for a weighted model. Throughout the modelling process for the Berlín geothermal field, data comparison, data combining, and evaluation of various data sets revealed, and confirmed different aspects of the latest conceptual model. However, it also revealed new aspects that help understand and characterize the geothermal reservoir in another way, resulting in new input to the discussion on problems in the reinjection and production areas influenced by the fluid-flow patterns and the structural system. Evaluating new drilling targets for production wells has been the focus of all models in the weighted model.

Available data have been interpreted and updated to a digital format to be integrated into a 3D model. The main 3D models are shown in this project together with their correlation and integration in the weighted model. Additionally, the modelling approach and methods are briefly discussed.

An advantage of the weighted model is the possibility to dynamically update it with new data. In addition, the results help lowering the risk of drilling.

5.2 Recommendations

- Update and calibrate the weighted model with new data and additional information from new production and injection wells in the favourable areas.
- Include detailed information on the deep geochemistry of the geothermal wells in the weighted model.
- Include the seismic tomography model in the weighted model to verify the location of the heat source and ascent zones of geothermal fluids.
- Priority areas 1, 2, 3, 4 and 5 are the most favourable as future drilling targets. In addition, areas 6, 7 and 8 could be considered as new exploration zones.

ACKNOWLEDGEMENTS

I want to thank GRÓ GTP for the opportunity to learn more about the beautiful world of geothermal energy, for all the support and care, for a lovely stay in Iceland, and for giving me many friends from different countries and cultures who have helped me to be more sociable and to learn more about different cultures and professional fields. Thank you, Guðni Axelsson, Málfríður Ómarsdóttir, Ingimar Haraldsson, and Vigdís Harðardóttir for your help and support.

Infinite thanks to my supervisor Gylfi Páll Hersir and my co-supervisors Bjarni Richter and Sveinborg Gunnarsdóttir for their support and sharing of their knowledge in developing my project. Thank you for being more than mentors, you also became my friends.

Thanks to my friends and family in El Salvador for all the support provided jn fulfilling this adventure of my professional life because, without them, this would not have been possible.

REFERENCES

Asunción, A., and Pabón, M., 2019: Methodological proposal for the social acceptance of geothermal projects of direct use in communities within zones of geothermal interest in El Salvador (in Spanish). *Geothermal Training for Latin America 2019. Universidad de El Salvador, El Salvador.*

Browne, P.R.L., 1978: Hydrothermal alteration in active geothermal fields. *Annual Reviews of Earth and Planetary Science, 6,* 229-250.

DeMets, C., 2001: A new estimate for present-day Cocos-Caribbean plate motion: Implications for slip along the Central American volcanic arc. *Geophysical Research Letters, 28(21),* 4043-4046. DOI:10.1029/2001GL013518.

Franzson, H., 2008: Chemical transport in geothermal systems in Iceland: Evidence from hydrothermal alteration. *Journal of Volcanology and Geothermal Research, 173*, 217-229.

Giao, P.H., Weller, A., Hien, D.H. and Adisornsupawat, K., 2008: An approach to construct the weathering profile in a hilly granitic terrain based on electrical imaging. *Journal of Applied Geophysics, 65(1),* 30-38.

Hersir, G.P., Guðnason, E.Á. and Flóvenz, Ó.G., 2022: Geophysical exploration techniques. In: Letcher, T., (ed.) *Comprehensive Renewable Energy – 2nd edition, Vol 7.,* Elsevier, Oxford. Available at: *https://doi.org/10.1016/B978-0-12-819727-1.00128-X*.

Kristmannsdóttir, H., 1979: Alteration of basaltic rocks by hydrothermal activity at 100-300°C. In: Mortland, M.M., and Farmer, V.C. (eds.), *International Clay Conference 1978*. Elsevier Scientific Publishing Co., Amsterdam, 359-367.

Kristmannsdóttir, H., 1985: The role of clay minerals in geothermal energy research. *Proceedings of Nordic Symposium, clay minerals-modern society,* 125-132.

LaGeo, 2007: *Reservoir engineering update for The Berlín Geothermal Field*. LaGeo, Santa Tecla, El Salvador, internal report.

LaGeo, 2011: *LaGeo sustainability Protocol report*. LaGeo, Unidad de Reservorios, Santa Tecla, unpublished report (in spanish).

LaGeo, 2018: *Tracer Test Report conducted in 2018 in TR-12A and TR-4A reinjection wells - Berlín Geothermal Field*. LaGeo, Santa Tecla, internal report (in Spanish).

LaGeo, 2019: *Conceptual model of the Berlín geothermal field, 2019*. LaGeo, Santa Tecla, internal report (in Spanish).

LaGeo, 2020a: *Annual Operation Report, Berlín Geothermal Power Plant, 2020*. LaGeo, Santa Tecla, El Salvador, internal report (in Spanish).

LaGeo, 2020b: *Sustainability and development of the Berlín geothermal field*. LaGeo, Santa Tecla, internal source (in Spanish).

LaGeo, 2021a: *Synthesis of potential of new geothermal areas.* LaGeo, Santa Tecla, internal source (in Spanish).

LaGeo, 2021b: *Maximum steam flow rate in the productor wells, period 2020-2021.* LaGeo, Santa Tecla, internal source (in Spanish).

LaGeo-SIGET (Superintendencia General de Electricidad y Telecomunicaciones), 2012: *Berlín Geothermal Field sustainability protocol: Calculation of the sustainable energy value Eo*. LaGeo and SIGET, Santa Tecla, internal report (in Spanish), 13 pp.

Leapfrog, 2021a: *What is implicit modelling?* website: *https://www.seequent.com/products-solutions/leapfrog-geothermal/.*

Leapfrog, 2021b: *Inverse Distance Weighted Grid Interpolants.* website: *https://help.seequent.com/Geothermal/4.1/en-GB/Content/interpolants/idw-interpolant.htm#:~:text=An%20IDW%20interpolant%20interpolates%20points,UBC%20grids%20and%20GOCAD%20models.*

Montalvo, F., and Axelsson. G., 2000: Assessment of chemical and physical reservoir parameters during six years of production-reinjection at Berlín Geothermal Field (El Salvador*). Proceedings of the World Geothermal Congress 2000, Ksushu-Tohoku, Japan,* 2153-2158.

Monterrosa, M., and Santos, P., 2013: Conceptual models for the Berlín Geothermal Field, case history. *Presented at "Short Course V on Conceptual Modelling of Geothermal Systems"*, *organized by UNU-GTP and LaGeo, Santa Tecla, El Salvador*, 9 pp.

Reyes, A.G., 2000: *Petrology and mineral alteration in hydrothermal systems: from diagenesis to volcanic catastrophes.* UNU-GTP, Iceland, report 18, 1998, 77 pp.

Rodriguez, V.A., 2005: Analysis of temperature and pressure measurements and production data for Berlín Geothermal Field, El Salvador. Report 16 in: *Geothermal Training in Iceland 2005*. UNU-GTP, Iceland, 297-332.

Shervais, J.W., Glen, J.M., Siler, D., Liberty, L.M., Nielson, D., Garg, S., Dobson, P., Gasperikova, E., Sonnenthal, E., Newell, D., Evans, J., DeAngelo, J., Peacock, J., Earney, T., Schermerhorn, W. and Neupane, G., 2020: Play Fairway analysis in geothermal exploration: The snake river plain volcanic province. *Proceedings of the 45th Workshop on Geothermal Reservoir Engineering, Stanford University, Stanford, California,* SGP-TR-216, 9 pp.

Unidad de Transacciones S.A. de C.V., 2020: *Annual Statistical Bulletin 2020 (in Spanish).* Unidad de Transacciones S.A. de C.V., Santa Tecla, El Salvador. website: *www.ut.com.sv.*

Wilson, S.H., 1960: *Physical and chemical investigation of Ketetahi Hot Springs*. The Geology of Tongariro Subdivision, D.R. Gregg. NZ Geological Survey Bulletin 40, Wellington, 124-144.